22. Funae,Y. and Imaoka,S. (1985) Simultaneous purification of multiple forms of rat liver microsomal cytochrome P-450 by high-performance liquid chromatography. *Biochim. Biophys. Acta*, **842**, 119–132.
23. Mason,R.P., Hanna,P.M., Burkitt,M.J. and Kadiiska,M.B. (1994) Detection of oxygen-derived radicals in biological systems using electron spin resonance. *Environ. Health Perspect.*, **102**, 33–36.
24. Omura,T. and Sato,R. (1964) The carbon monoxide binding pigment of liver microsomes. *J. Biol. Chem.*, **239**, 2370–2378.
25. Sonderfan,A.J., Arlotto,M.P., Dutton,D.R., McMillen,S.K. and Parkinson,A. (1987) Regulation of testosterone hydroxylation by rat liver microsomal cytochrome P-450. *Arch. Biochem. Biophys.*, **15**, 27–41.
26. Kitada,M., Komori,M., Ohi,H., Imaoka,S., Funae,Y. and Kamataki,T. (1989) Form-specific degradation of cytochrome P-450 by lipid peroxidation in rat liver microsomes. *Res. Commun. Chem. Pathol. Pharmacol.*, **63**, 175–88.
27. Laemmli,U.K. (1970) Cleavage of structural proteins during the assembly of the head of bacteriophage T4. *Nature*, **227**, 680–685.
28. Dutton,D.R., Reed,G.A. and Parkinson,A. (1989) Redox cycling of resorufin catalyzed by rat liver microsomal NADPH-cytochrome P-450 reductase. *Arch. Biochem. Biophys.*, **268**, 605–616.
29. Kasai,H., Crain,P.F., Kuchino,Y., Nishimura,S., Ootsuyama,A. and Tanooka,H. (1986) Formation of 8-hydroxyguanine moiety in cellular DNA by agents producing oxygen radicals and evidence for its repair. *Carcinogenesis*, **7**, 1849–1851.
30. Imaida,K., Tatematsu,M., Kato,T., Tsuda,H and Ito,N. (1989) Advantages and limitations of stereological estimation of placental gluthathione *S*-transferase-positive rat liver cell foci by computerized three-dimensional construction. *Jpn. J. Cancer Res.*, **80**, 326–330.
31. Watanabe,I., Toyoda,M., Okuda,J., Tenjo,T., Tanaka,K., Yamamoto,T., Kawasaki,H., Sugiyama,T., Kawarada,Y. and Tanigawa,N. (1999) Detection of apoptotic cells in human colorectal cancer by two different *in situ* methods: antibody against single-stranded DNA and terminal deoxynucleotidyl transferase-mediated dUTP-biotin nick end-labeling (TUNEL) methods. *Jpn. J. Cancer Res.*, **90**, 180–193.
32. Chomzynski,P. (1993) A reagent for the single-step simultaneous isolation of RNA, DNA and proteins from cell and tissue samples. *Focus*, **15**, 532–536.
33. Sugimura,K., Lee,C.C.R., Kim,T., Goto,T., Kasai,S., Harimoto,K., Yamagami,S. and Kishimoto,T. (1997) Production of hepatocyte growth factor is increased in chronic renal failure. *Nephron*, **75**, 7–12.
34. Szabo,G., Kartarova,Z., Hoertnagl,B., Somogyi,R. and Sperk,G. (2000) Differential regulation of adult and embryonic glutamate decarboxylases in rat dentate granule cells after kainite-induced limbic seizures. *Neuroscience*, **100**, 287–295.
35. Nishikawa,T., Wanibuchi,H., Ogawa,M., Kinoshita,A., Morimura,K., Hiroi,T., Funae,Y., Kishida,H., Nakae,D. and Fukushima,S. (2002) Promoting effects of monomethylarsonic acid, dimethylarsinic acid and trimethylarsine oxide on induction of rat liver preneoplastic glutathione *S*-transferase placental form positive foci: a possible reactive oxygen species mechanism. *Int. J. Cancer*, **100**, 136–139.
36. Shimada,M., Murayama,N., Yamauchi,K., Yamazoe,Y. and Kato,R. (1989) Suppression in the expression of a male-specific cytochrome P450, P450-male: difference in the effect of chemical inducers on P450-male mRNA and protein in rat livers. *Arch. Biochem. Biophys.*, **270**, 578–587.
37. Shibutani,S., Takeshita,M. and Grollman,A.P. (1991) Insertion of specific bases during DNA synthesis past the oxidation-damaged base 8-oxodG. *Nature*, **349**, 431–434.
38. Denda,A., Endoh,T., Nakae,D. and Konishi,Y. (1995) Effects of oxidative stress induced by redox-enzyme modulation on rat liver hepatocarcinogenesis. *Toxicol. Lett.*, **82–83**, 413–417.
39. Fraga,C.G., Shigenaga,M.K., Park,J.W., Degan,P. and Ames,B.N. (1990) Oxidative damage to DNA during aging: 8-hydroxy-2′-deoxyguanosine in rat organ DNA and urine. *Proc. Natl Acad. Sci. USA*, **87**, 4533–4537.
40. Lawrence,J.M. (2000) Oxyradicals and DNA damage. *Carcinogenesis*, **21**, 361–370.
41. Kondo,S., Toyokuni,S., Tanaka,T., Hiai,H., Onodera,H., Kasai,H. and Imamura,M. (2000) Overexpression of the *hOGG1* gene and high 8-hydroxy-2′-deoxyguanosine (8-OHdG) lyase activity in human colorectal carcinoma: regulation mechanism of 8-OHdG level in DNA. *Clin. Cancer Res.*, **6**, 1394–1400.
42. Biju,M.P., Pyroja,S., Rajeshkumar,N.V. and Paulose,C.S. (2001) Hepatic GABA-A receptor functional regulation during rat liver cell proliferation. *Hepatol. Res.*, **21**, 136–146.
43. Erlitzki,R., Gong,Y., Zhang,M. and Minuk,G. (2000) Identification of gamma-aminobutyric acid receptor subunit types in human and rat liver. *Am. J. Physiol. Gastrointest. Liver Physiol.*, **279**, G733–799.
44. Biju,M.P., Pyroja,S, Rajeshkumar,N.V. and Paulose,C.S. (2002) Enhanced GABA(B) receptor in neoplastic rat liver: induction of DNA synthesis by baclofen in hepatocyte cultures. *J. Biochem. Mol. Biol. Biophys.*, **6**, 209–214.
45. Kolaja,K.L., Stevenson,D.E., Walborg,F. and Klaunig,J.E. (1996) Dose dependence of phenobarbital promotion of preneoplastic hepatic lesions in F344 rats and B6C3F1 mice: effects on DNA synthesis and apoptosis. *Carcinogenesis*, **5**, 67–71.
46. Ueda,A., Hamadeh,H.K., Webb,H.K., Yamamoto,Y., Sueyoshi,T., Afshari,C.A., Lehmann,J.M. and Negishi,M. (2002) Diverse roles of the nuclear orphan receptor CAR in regulating hepatic genes in response to phenobarbital. *Mol. Pharmacol.*, **61**, 1–6.
47. Dhanasekaran,N. and Prasad,M.V. (1998) G protein subunits and cell proliferation. *Biol. Signals Recept.*, **7**, 109–117.
48. Gonzales,A.J., Christensen,J.G., Preston,R.P., Goldsworthy,T.L., Tlsty,T.D. and Fox,T.R. (1998) Attenuation of G_1 checkpoint function by the non-genotoxic carcinogen phenobarbital. *Carcinogenesis*, **19**, 1173–1183.
49. Martens,U., Lennartsson,P., Hogberg,J. and Stenius,U. (1996) Low expression of the WAF1/CIP1 gene product, p21, in enzyme-altered foci induced in rat liver by diethylnitrosamine or phenobarbital. *Cancer Lett.*, **104**, 21–26.
50. Christensen,J.G., Romach,E.H., Healy,L.N., Gonzales,A.J., Anderson,S.P., Malarkey,D.E., Corton,J.C., Fox,T.R., Cattley,R.C. and Goldsworthy,T.L. (1999) Altered bcl-2 family expression during non-genotoxic hepatocarcinogenesis in mice. *Carcinogenesis*, **20**, 1583–1590.
51. Christensen,J.G., Goldsworthy,T. and Cattley,R.C. (1999) Dysregulation of apoptosis by *c-myc* in transgenic hepatocytes and effects of growth factors and non-genotoxic carcinogens. *Mol. Carcinogen.*, **25**, 273–284.
52. Hagiwara,A., Matsuda,T., Tamano,S., Kitano,M., Imaoka,S., Funae,Y., Takesada,Y., Shirai,T. and Fukushima,S. (1996) Dose-related increases in quantitative values for altered hepatocytic foci and cytochrome P-450 levels in rats exposed to phenobarbital in a medium-term bioassay. *Cancer Lett.*, **110**, 155–162.

Received October 15, 2002; revised April 22, 2003; accepted April 23, 2003

Cell, Vol. 113, 905–917, June 27, 2003, Copyright ©2003 by Cell Press

The Chromatin-Remodeling Complex WINAC Targets a Nuclear Receptor to Promoters and Is Impaired in Williams Syndrome

Hirochika Kitagawa,[1,2] Ryoji Fujiki,[1] Kimihiro Yoshimura,[1] Yoshihiro Mezaki,[1] Yoshikatsu Uematsu,[1] Daisuke Matsui,[1] Satoko Ogawa,[1] Kiyoe Unno,[1,3] Mataichi Okubo,[3] Akifumi Tokita,[3] Takeya Nakagawa,[4] Takashi Ito,[4] Yukio Ishimi,[5] Hiromichi Nagasawa,[5] Toshio Matsumoto,[2] Junn Yanagisawa,[1,7] and Shigeaki Kato[1,7,*]

[1]Institute of Molecular and Cellular Biosciences
University of Tokyo
1-1-1 Yayoi
Bunkyo-ku
Tokyo 113-0032
Japan

[2]First Department of Internal Medicine
University of Tokushima School of Medicine
3-18-15 Kuramoto-cho
Tokushima 770-8503
Japan

[3]Department of Pediatrics
Juntendo University School of Medicine
3-1-3 Hongo
Bunkyo-ku
Tokyo 113-8431
Japan

[4]Department of Biochemistry
Nagasaki University School of Medicine
1-12-4 Sakamoto
Nagasaki 852-8523
Japan

[5]Mitsubishi Kagaku Institute of Life Sciences
11 Minamiooya
Machida-shi
Tokyo 194-8511
Japan

[6]Department of Applied Biological Chemistry
Graduate School of Agricultural and Life Sciences
University of Tokyo
1-1-1 Yayoi
Bunkyo-ku
Tokyo 113-0032
Japan

[7]SORST
Japan Science and Technology
4-1-8 Honcho
Kawaguchi
Saitama 332-0012
Japan

Summary

We identified a human multiprotein complex (WINAC) that directly interacts with the vitamin D receptor (VDR) through the Williams syndrome transcription factor (WSTF). WINAC has ATP-dependent chromatin-remodeling activity and contains both SWI/SNF components and DNA replication-related factors. The latter might explain a WINAC requirement for normal S phase progression. WINAC mediates the recruitment of unliganded VDR to VDR target sites in promoters, while subsequent binding of coregulators requires ligand binding. This recruitment order exemplifies that an interaction of a sequence-specific regulator with a chromatin-remodeling complex can organize nucleosomal arrays at specific local sites in order to make promoters accessible for coregulators. Furthermore, overexpression of WSTF could restore the impaired recruitment of VDR to vitamin D regulated promoters in fibroblasts from Williams syndrome patients. This suggests that WINAC dysfunction contributes to Williams syndrome, which could therefore be considered, at least in part, a chromatin-remodeling factor disease.

*Corresponding author: uskato@mail.ecc.u-tokyo.ac.jp

Introduction

Lipophilic ligands, such as fat-soluble vitamins A/D and thyroid/steroid hormones, exert their actions through transcriptional control of particular sets of target genes by direct binding and consequent activation of their cognate nuclear receptors (NRs) (Mangelsdorf et al., 1995). NRs form a superfamily and act as ligand-inducible regulators. From their functional and structural similarities, NR proteins are divided into five functional domains, designated A to E. The ligand binding domain (LBD) is located in the C-terminal E domain. The most conserved domain, C, is located in the NR center and serves as the DNA binding domain to specifically recognize and directly bind to their cognate ligand response elements in the target promoters. The LBD also harbors ligand-inducible transactivation function (AF-2). Upon ligand binding, NRs control transcription through ligand-dependent associations with a number of coregulators and coregulator complexes (Glass and Rosenfeld, 2000).

At transcriptional initiation sites in promoters, distinct classes of multiprotein complexes are thought to be indispensable for controlling transcription of sequence-specific regulators (Emerson, 2002; Narlikar et al., 2002). These complexes modify the chromatin configuration in a highly regulated manner, like nucleosome rearrangement, and bridge the functions between regulators and basal transcription factors, along with RNA polymerase II. Two major classes of chromatin-modifying complexes have been well characterized and their anchoring to the promoters presumably requires enzyme-catalyzed modifications of histone tails in chromatin (Hassan et al., 2002). One class contains several discrete subfamilies of transcription coregulatory complexes with either histone acetylase (HAT) or histone deacetylase (HDAC) activities to covalently modify histones through acetylation. In NR

ligand-induced transactivation processes, the complexes containing HDAC first act to corepress transactivation of unliganded NRs, while upon ligand binding, two HAT complexes, p160/CBP and TRRAP/GCN5, coactivate the NR function, like the other non-HAT DRIP/TRAP/SMCC coactivator complexes (Onate et al., 1995; Kamei et al., 1996; Rachez et al., 1998; Gu et al., 1999; Yanagisawa et al., 2002).

Another class of complexes uses ATP hydrolysis to rearrange nucleosomal arrays in a noncovalent manner and render chromosomal DNA accessible for sequence-specific regulators (Narlikar et al., 2002). These ATP-dependent chromatin-remodeling complexes act on transcription, DNA repair, and DNA replication and have been classified into subfamilies based on the major catalytic components with ATPase activity, SWI2/SNF2, ISWI, and Mi-2 (Fyodorov and Kadonaga, 2001; Yasui et al., 2002). These ATPases are highly conserved from yeast to humans and each forms a functionally similar, but distinct complex with a combination of specific components. However, the roles of most of the other components, except the catalytic subunits in chromatin remodeling, remain largely unknown (Narlikar et al., 2002).

Accumulating evidence revealed that both the chromatin-remodeling complexes and the coregulatory complexes cooperatively support transactivation of sequence-specific regulators like NRs (Glass and Rosenfeld, 2000; Emerson, 2002; Narlikar et al., 2002). However, the underlying molecular basis of the functional interplay among the complexes and the order of their recruitment through regulators to the promoters in controlling transcription at the specific local sites on the promoters are largely unknown.

Williams syndrome (WS) is a rare autosomal dominant hereditary disorder with multiple symptoms, including typically congenital vascular lesion, elfin face, mental retardation, and growth deficiency (Lu et al., 1998). Transient appearance of infantile aberrant vitamin D metabolism and hypercalcemia in the WS patients was also documented (Taylor et al., 1982; Garabedian et al., 1985). This syndrome is associated with genetic deletions at chromosome 7q 11.23, and several candidate genes in the deleted regions have been mapped from their mRNA expression levels (Hoogenraad et al., 2002). One gene, the Williams syndrome transcription factor (WSTF), has been suspected to be a candidate responsible for the diverse WS disorders (Lu et al., 1998; Peoples et al., 1998). This possibility is raised by the fact that WSTF is highly homologous to hACF1 as one of the WAC family proteins (Jones et al., 2000). Also, hACF1 is a partner of hSNF2h (a *Drosophila* ISWI homolog) to form well-characterized ISWI-based chromatin-remodeling complexes (Poot et al., 2000).

To search a chromatin-modifying complex to account for the ligand-independent occupancy of VDR in the target promoters, we purified from MCF7 cells a human multiprotein complex named "WINAC". The analysis of WINAC represents not only a molecular mechanism that a direct and selective interaction of a sequence-specific regulator with a chromatin-remodeling complex, but also the relationship between the function of WINAC and Williams syndrome disorders.

Results

Purification of a WSTF-Containing Multiprotein Complex Interacting with the VDR Ligand Binding Domain

To identify a coregulator complex for nuclear receptors, HeLa cell nuclear extracts were incubated with a chimeric VDR-DEF region protein (VDR-DEF) fused to glutathione-S-transferase (GST), in the presence or absence of 1α,25(OH)2D3 (Figure 1A). Proteins associated with VDR were collected under a milder washing condition (Yanagisawa et al. 2002) than that in the previous report (Rachez et al., 1998). Proteins that interacted with VDR-DEF were separated by SDS-PAGE and silver stained (Figure 1B). Mass spectrometry and the apparent molecular weights of the different proteins associated with the VDR-DEF in a ligand-dependent way led to the identification of several known components of the DRIP/TRAP/SMCC complex (Figure 1B), in agreement with previous observations (Rachez et al., 1998; Gu et al., 1999; Yanagisawa et al., 2002). One of the ligand-independent VDR-specific interactants was the Williams syndrome transcription factor (WSTF)/WBSCR9/BAZ1B (Lu et al., 1998; Peoples et al., 1998; Jones et al., 2000) (Figure 1B), and the WSTF protein was detected indeed in native HeLa cells (Figure 1C).

By Western blotting with specific antibodies, the NR coactivators, TRAP220 and TIF2, were detected only when VDR and ERα were liganded (Figure 1B). Unlike these factors, no ligand dependency, but VDR-selective interaction was found in WSTF (Figure 1B). By a GST pull-down assay, the physical and constitutive interaction of recombinant WSTF in vitro was observed for VDR-DEF irrespective of ligand binding, but not detected for ERα LBD (Figure 1D). In coimmunoprecipitations using the nuclear extracts of transfected MCF7 cells, WSTF appeared to interact with both unliganded and liganded VDR, while ligand-dependent recruitment of TRAP220 and TIF2 were expectedly seen for VDR as well as ERα (Yanagisawa et al., 2002) (Figure 1E).

To purify a WSTF-containing complex, we established a MCF7 stable transformant overexpressing FLAG-tagged WSTF. With the nuclear extracts of the stable transformants, WSTF containing complexes were isolated by multistep purification using the GST-VDR column and an anti-FLAG affinity resin column (Figure 2A). On the glycerol density gradient (Figure 2B, upper image), the purified complexes with a molecular weight of greater than 670 kDa bound to the GST-VDR column and these large molecular weight fractions contained WSTF, indicating that WSTF forms a stable nuclear complex. The fractions containing FLAG-tagged WSTF were then applied on the anti-FLAG affinity column to isolate the complex.

Identification of a WSTF Complex

With the mass fingerprinting, we identified all the components of the purified complex containing WSTF (Figure 2C), and designated this complex as WINAC (*W*STF *I*ncluding *N*ucleosome *A*ssembly *C*omplex). WINAC stable formation was further supported by coimmunoprecipitation with a CAF-1p150 antibody (Figure 2C). WINAC consists of at least 13 components, but unexpectedly

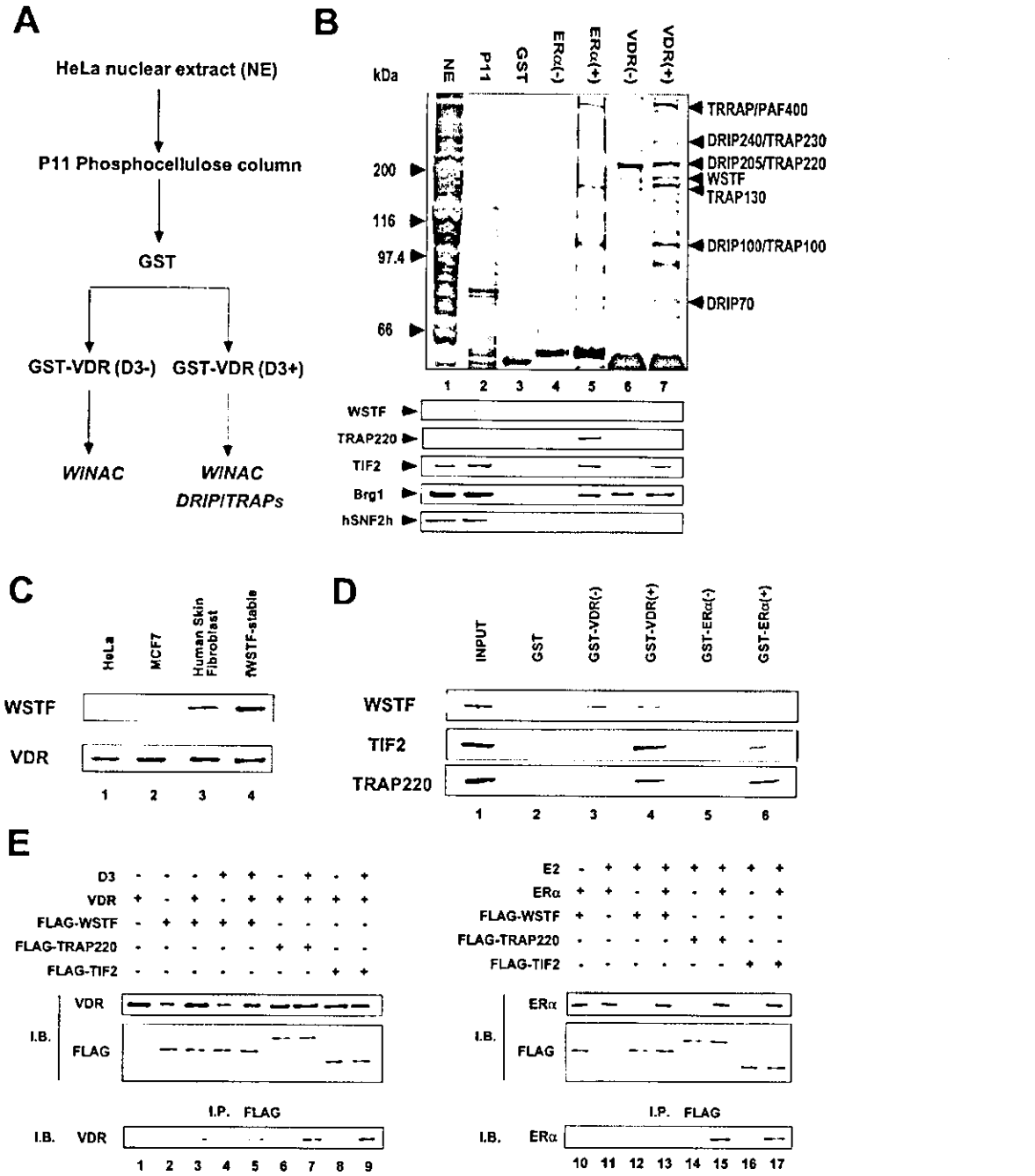

Figure 1. Purification and Identification of Human Proteins Interacting with 1α,25(OH)2D3, Unbound and Bound VDR

(A) Purification scheme for VDR interacting proteins. The eluted fraction from P11 phosphocellulose column was incubated with immobilized GST-VDR(DEF) in the absence or presence of 1α,25(OH)2D3(D3,10^{-6} M).

(B) Identification of ligand-independent and -dependent VDR interacting proteins. In the upper image, fractions were subjected to SDS-PAGE, followed by silver staining. Total HeLa S3 nuclear extract [NE] (lane 1), a fraction eluted from the P11 column [p11] (lane 2), fractions from GST [GST] (lane 3), unliganded- and liganded-GST-ERα(DEF) columns [ERα(−);ERα(+)] (lanes 4 and 5), unliganded- and liganded-GST-VDR(DEF) columns [VDR(−);VDR(+)] were examined by mass spectrometry and identified proteins are indicated at the right side of the image. The lower image shows Western blot analysis using specific antibodies shown in the image.

(C) Protein expression in cultured cells. Western blotting with antibodies against WSTF or VDR was performed with indicated cell lines (3 × 10^6 cells/lane).

(D) Direct and ligand-independent interaction of WSTF with VDR in vitro. WSTF, TIF2, and TRAP220 were translated in vitro and incubated with a receptor-GST chimeric protein immobilized on glutathione-Sepharose beads in the presence or absence of the cognate ligands.

(E) 1α,25(OH)2D3-independent interaction between VDR and WSTF in vivo. The upper image displays the Western blot of the total cell extracts (Yanagisawa et al., 2002) to verify expression. The lower image shows the Western blot of the immunoprecipitates by anti-FLAG M2-affinity resin to detect the receptor.

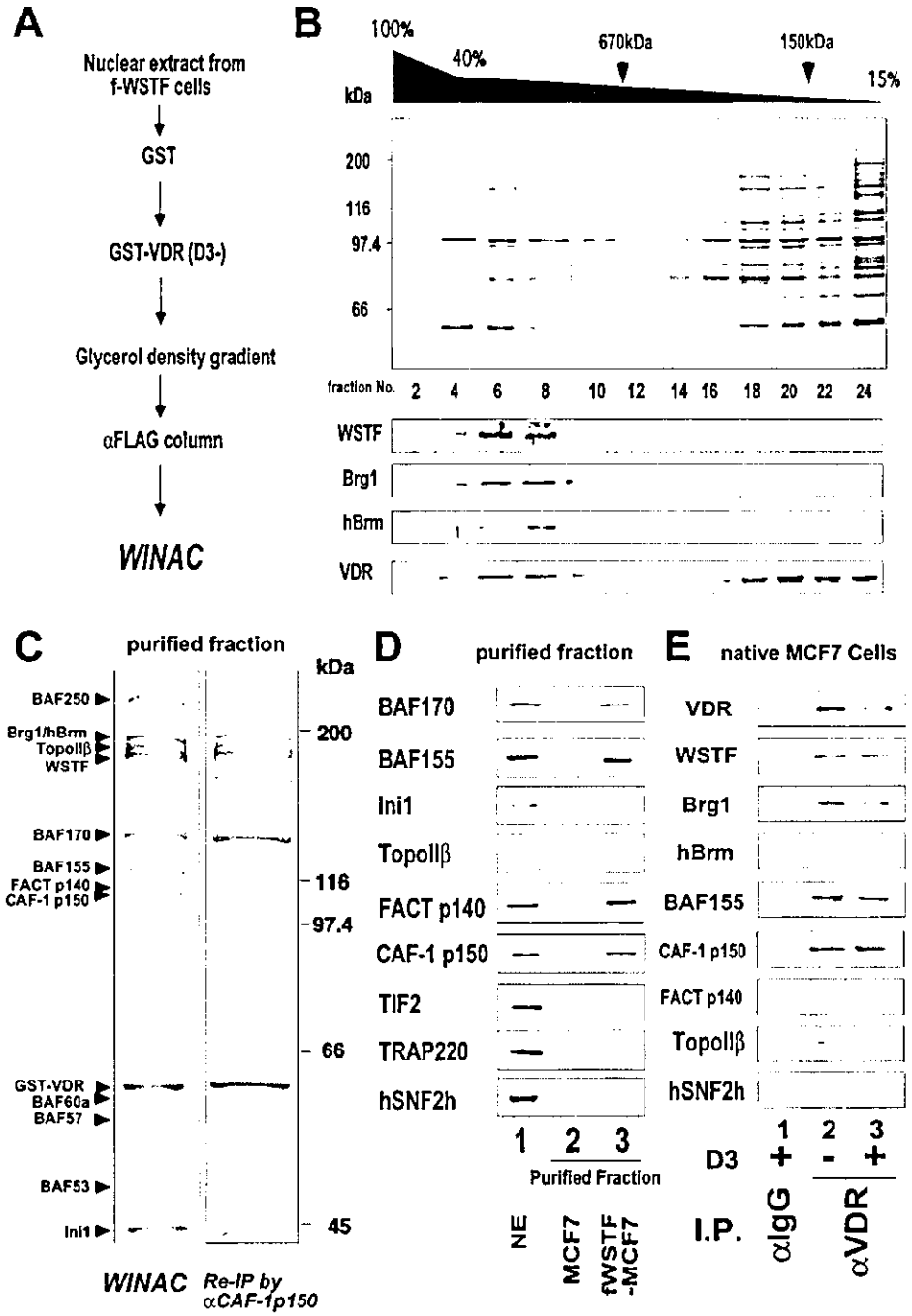

Figure 2. Purification and Identification of a Human WSTF-Containing Multiprotein Complex "WINAC"

(A) Purification scheme of WINAC from MCF7 stable transformants (Yanagisawa et al., 2002).

(B) Fractionation of purified complexes on glycerol density gradient. In the lower image, Western blot analysis of each fraction using specific antibodies is shown.

(C) The purified complex was subjected to SDS-PAGE, followed by silver staining and identified by mass spectrometry (left image). The right image shows the reimmunoprecipitation (Re-IP) of purified WINAC by the anti-CAF-1 p150 antibody.

(D) Western blot analysis of WINAC. Western blot analysis was performed to compare nuclear extracts (lane 1), mock MCF7 (lane 2), and FLAG-WSTF stable transformants containing WINAC (lane 3) with specific antibodies.

(E) Detection of endogenous WINAC components by Western blotting.

contains neither hSNF2h nor the components of known ISWI-based complexes (Figure 2C). Rather, the SWI/SNF type ATPases (Brg1 and hBrm) and several BAF components share with the SWI2/SNF2-based complexes (Narlikar et al., 2002). However, we could not detect BAF180, which is specific to one of the hSWI/

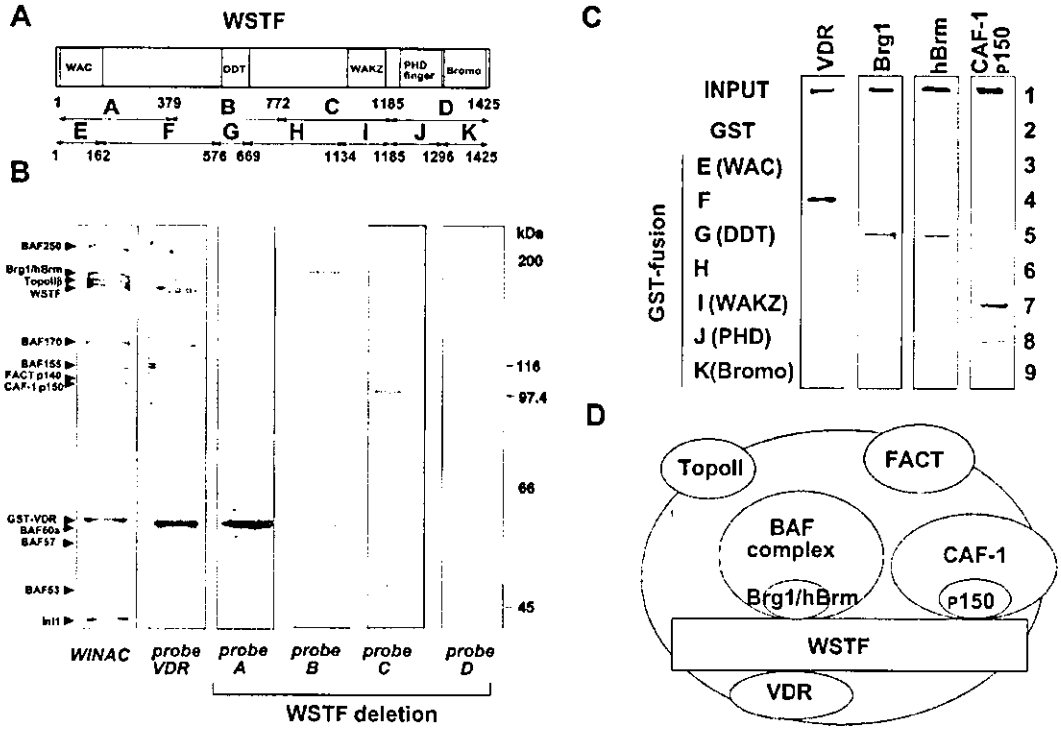

Figure 3. WSTF as a Platform Protein in WINAC

(A) Schematic representation of the probes used for the Far Western blotting and the GST pull-down assay. WSTF deletion mutants are expressed as GST-chimeric proteins.

(B) Far Western blotting of the WINAC complex probed with indicated ^{32}P-labeled GST-fused chimeric proteins. ^{32}P-labeled GST-fused chimeric proteins were prepared with pGEX-2TK vector (Amersham Biosciences) by PKA phosphorylation (Rachez et al., 1998).

(C) Physical interaction of WINAC components and VDR with WSTF deletion mutants in GST pull-down assay.

(D) Schematic representation of the interacting domains of WSTF.

SNF-type complexes, PBAF, which was purified and identified by in vitro transcription to coactivate VDR in a ligand-dependent manner (Lemon et al., 2001). Interestingly, WINAC appears to harbor three components (TopoIIβ, FACTp140, and CAF-1p150) (Smith and Stillman, 1989; Varga-Weisz et al., 1997; LeRoy et al., 1998), which have not yet been found in any known ATP-dependent chromatin-remodeling complexes. Western blotting with specific antibodies verified several WINAC components (Figure 2D). Moreover, major WINAC components in a purified endogenous complex associating with VDR were detected (Figure 2E), supporting presence of WINAC as a stable complex in native cells.

Clear retention of VDR was detected upon the WSTF band, but not the other subunits (Figure 3B), confirming the GST-pull-down assay results (Figure 1D). The WSTF fragments were trapped on not only VDR but also CAF-1p150 and Brg1/hBrm (Figure 3B). Such interactions were also seen in the expected regions by the GST-pull-down assay (Figure 3C), suggesting that WSTF serves as a platform subunit to assemble components into WINAC (as illustrated in Figure 3D).

WINAC Is a Multifunctional ATP-Dependent Chromatin-Remodeling Complex

We then examined if purified WINAC exerts an ATP-dependent chromatin-remodeling activity by comparing its activity with a complex of the recombinant dAcf1 and dISWI proteins in a standard micrococcal nuclease assay. This recombinant complex has been reported sufficient to mobilize nucleosomes in vitro in an ATP-dependent manner (Ito et al., 1997). Like the dISWI complex, an ATP-dependent chromatin-assembly reaction was clearly induced by WINAC (compare lanes 6, 7, and lane 3 in Figure 4A), indicating that Brg1/hBrm in WINAC serves as an ATPase for this ATP-dependent chromatin-remodeling process. WINAC appeared to have a chromatin-assembly activity (data not shown) like RSF (Loyola et al., 2001).

We then examined the ability of WINAC to disrupt nucleosome arrays through VDR bound DNA since the known ATP-dependent chromatin-remodeling complexes are potent to recognize the nucleosomal array around the binding sites of a sequence-specific regulator (Ito et al., 1997; Lemon et al., 2001). By Southern blot analysis with a pair of oligonucleotides complementary to a region in the vicinity (promoter probe) or to a site about 900 bp upstream (distal probe) of the GAL4 DBD binding sites for a chimeric VDR-DEF protein (GAL-VDR), disruption of the nucleosome arrays in the GAL4 binding site vicinity was induced only when both VDR and WINAC were present (lane 4 in Figure 4B), while the other regions appeared unaffected in the nucleosome arrays (Figure 4B). Reflecting the VDR-specific nucleo-

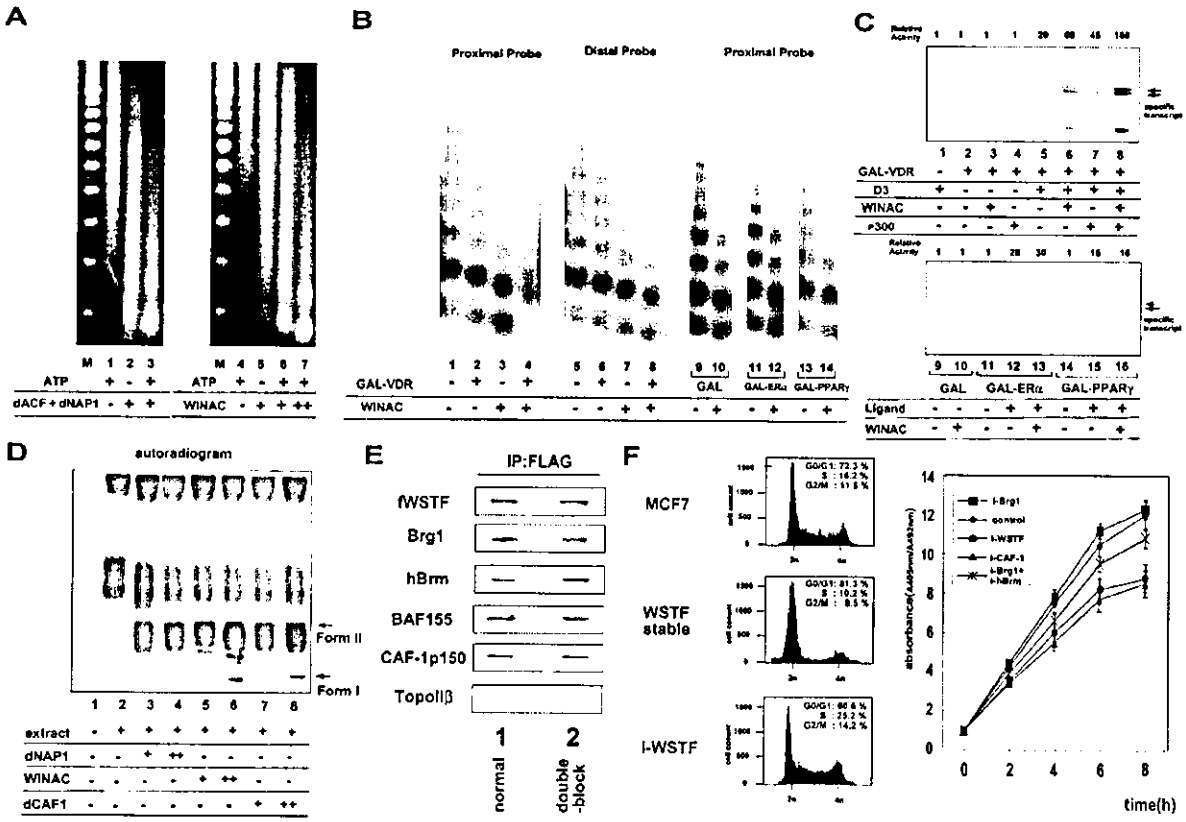

Figure 4. WINAC as an ATP-Dependent Chromatin-Remodeling Complex

(A) Chromatin-reconstitution activity of WINAC. The reacted samples were subjected to partial micrococcal nuclease digestion. The molecular mass marker (M) is the 200 bp ladder.

(B) Chromatin disruption by WINAC is specifically VDR dependent. Oligonucleotide probe corresponds to either a sequence between the GAL4 sites and the RNA start site (proximal probe) or 900 bp upstream of the start site (distal probe).

(C) Potentiation of VDR transactivation by WINAC in vitro. Arrows indicate specific transcripts by transcription reactions by GAL4 derivatives. A representative result is displayed, and relative activities were calculated from three independent assays with pGI0 vector as an internal control.

(D) WINAC functions as a chromatin-reconstitution factor during DNA replication in vitro. During DNA replication induced by SV40 T antigen in vitro, WINAC could form chromatin with negatively supercoiled DNA. Form I, a perfect supercoiled DNA; form II, a relaxed form.

(E) WINAC formation is unchanged in S phase. MCF7 stable transformants were cultured under either normal conditions or double-thymidine block treatments.

(F) Modulation of the cell cycle by altered WSTF expression. Left image: DNA histogram of the MCF7 cells [MCF7], WSTF stably expressing MCF7 cells [WSTF stable] and MCF7 cells transfected with WSTF-RNAi [i-WSTF]. Right image: BrdU incorporation during S phase of the MCF7 cells transfected with RNAi from the indicated proteins during double-thymidine treatment. After the final release (time 0), cells were collected every 2 hr, for up to 8 hr. The average values of triplicate analyses are shown.

some disruption by WINAC among tested receptors (Figure 4B), ligand-induced transactivation in vitro was potentiated by WINAC for VDR, but for neither ERα nor PPARγ (Figure 4C).

WINAC Function during DNA Replication

The WINAC function in DNA replication (Smith and Stillman, 1989; Varga-Weisz et al., 1997) was addressed by reconstituting chromatin structure upon newly replicated DNA by an in vitro assay. WINAC, like the reported CAF-1 histone chaperone complex (see lanes 7 and 8 in Figure 4D), could facilitate forming chromatin structure with negatively supercoiled DNA on newly replicated DNA through nucleosome arrangement (Smith and Stillman, 1989) (Figure 4D). Moreover, WINAC complex formation was detected irrespective of the cell-cycle stages, even when blocked at S stage by double-thymidine treatments (Fujita et al., 1996) (Figure 4E). Manipulation of WSTF expression by WSTF-RNAi expression (Elbashir et al., 2001) resulted in alterations in the cell cycle (left images in Figure 4F). Particularly, DNA synthesis was clearly lowered by RNAi expression of either WSTF or Brg1/hBrm ATPases (right image in Figure 4F). Thus, these findings suggest that WINAC plays a role in chromatin remodeling during DNA replication.

WSTF Coactivated Ligand-Induced Transactivation Function of VDR

Next, we investigated if WSTF potentiates the ligand-induced transactivation of VDR in MCF7 cells by transient expression analysis. 1α,25(OH)2D3 (10^{-9} M) was effective to induce VDR AF-2 transactivation function.

WSTF coactivated this ligand-induced AF-2 function of VDR, but not ERα (compare lanes 3 and 4 with 23 and 24 in Figure 5A). Both Brg1 and hBrm were potent to enhance the transactivation functions of VDR and ERα (compare lanes 9 and 12 with lane 2 for VDR; lanes 29 and 32 with lane 22 for ERα in Figure 5A) as previously reported (Chiba et al., 1994; DiRenzo et al., 2000; Shang et al., 2000; Belandia et al., 2002). Interestingly, such coactivator-like activity of WSTF was selective for VDR, and not detected for ERα, even in the presence of Brg1/hBrm (see lanes 30 and 33 in Figure 5A).

To confirm such a coactivator-like function of WSTF for VDR, the ligand-induced transactivation function of VDR was assessed 40 hr after the RNAi transfection and was severely attenuated nearly to basal transcription levels (lanes 7 and 8 in Figure 5A). Interestingly, WSTF-RNAi expression was found to also abrogate the VDR coactivation of the VDR transcriptional activity by the known NR coactivators, such as TRAP220 and TIF2 (lanes 16 and 18 in Figure 5A). Similarly, RNAi expression resulted in a loss of the coactivator-like function of WSTF for VDR when intact VDR/RXR heterodimer was bound to a naturally occurring positive vitamin D response element (VDRE) derived from the human 1α,25-dihydroxyvitamin D3 24-hydroxylase [24(OH)ase] gene promoter (Chen and DeLuca, 1995) (Figure 5C). ChIP analysis revealed that VDR and the WINAC components were constitutively associated with the promoter irrespective of ligand binding. In the contrast, ligand-induced occupancy in the promoter was seen in TRAP220 and TIF2 with ligand-induced histone H4 acetylation (compare lane 3 with 4 in Figure 5B), though the ligand-induced TRAP220 and TIF2 occupancy was cyclic (data not shown) as expected from previous reports (Shang et al., 2000). Such ligand-dependent and -independent recruitments of factors to the promoter were robustly attenuated by WSTF-RNAi expression (lane 5 in Figure 5B).

As the VDR/RXR heterodimer also represses transcription in a ligand-dependent manner through negative VDRE (nVDRE), the action of WSTF in the ligand-induced transrepression was examined in a naturally occurring nVDRE in human 25-hydroxyvitamin D3 1α-hydroxylase [1α(OH)ase] (Murayama et al., 1998). ChIP analysis uncovered that VDR and WINAC appear to land on the nVDRE in a ligand-independent manner, while ligand-induced (compare lane 8 with 9 in Figure 5B), but cyclic (data not shown) recruitments of N-CoR and HDAC2 were observed. Ligand-dependent repression was exaggerated by WSTF overexpression (lanes 3 and 4 in Figure 5D), but attenuated again by WSTF-RNAi expression (lanes 5 and 6 in Figure 5D). Thus, it is likely that WINAC association with VDR facilitates targeting of a putative corepressor complex to the nVDRE. The WINAC function in the native VDR target gene promoters and the endogenous gene expressions of 24(OH)ase and 1α(OH)ase were further confirmed by the impaired 1α,25(OH)2D3 responsiveness by the WSTF ablation (Figure 5E). Thus, these findings point out that WINAC rearranges the nucleosome array around the positive and negative VDREs, thereby facilitating the coregulatory complexes accessible to VDR for further transcription control.

Impaired Transactivation Function of VDR Was Recovered by WSTF Overexpression in Williams Syndrome Patients

Together with these observations, the typical phenotypes of the WSTF gene-deleted WS patients (Taylor et al., 1982; Garabedian et al., 1985) prompted us to assume that a lowered WINAC function caused by reduced WSTF expression may result in aberrant chromatin remodeling, leading to diverse abnormalities, including abnormal vitamin D metabolism and hypercalcemia. Considering WSTF and VDR skin expression (Yoshizawa et al., 1997), we first assessed the ligand-induced transactivation function of VDR in skin fibroblast cells derived from three normal and three WS patients, in which the region covering the WSTF gene is deleted in one chromosome 7 allele, as representatively shown in patient #1 by FISH analysis (Figure 6A). Northern blot analysis unmasked the WSTF expression levels were clearly lowered (~50%) in the WS patients (Figure 6B). By a transient transfection assay in fibroblast cells, we found reduced transactivation function of VDR in the WS patient cells (Figure 6C). Consistent with the impaired function of VDR in the WS cells, the ChIP analysis showed robust reduction in targeting of VDR, the WINAC components, and the coactivators to the 24(OH)ase VDRE (lanes 9 and 10 in Figure 6E), in agreement with the MCF7 cell results (Figure 5B).

Most strikingly, WSTF expression by an adenovirus vector (Kitagawa et al., 2002) could rescue the reduced responsiveness of 24(OH)ase gene induction by 1α,25(OH)2D3 for 12 hr in the WS skin fibroblasts (compare lane 3 with 4 in Figure 6D), with the impaired promoter targeting of the WINAC components and unliganded recoveries in VDR to the 24(OH)ase promoter (see lane 11 in Figure 6E), and the impaired ligand-induced recruitment of the NR coactivators (see lane 12 in Figure 6). Thus, these findings suggest that at least a part of the endocrine disorders found in the WS patients are related to VDR malfunction caused by the lowered WINAC function, which is due to lower WSTF expression.

The WSTF transcript during embryogenesis was not detected by Northern blotting, but detectable by RT-PCR (Figure 7A). By whole mount in situ staining (Sekine et al., 1999) at 9.5 dpc, the WSTF transcript appeared to be ubiquitously expressed (data not shown), but its expression pattern became limited and partially overlapped with mouse Brg1 and BAF155 (Srg3) expression (Bultman et al., 2000; Kim et al., 2001) as evident at 11.5 dpc (Figure 7B). Surprisingly these expression patterns seem different from that of mouse Snf2h (Lazzaro and Picketts, 2001), particularly at brain. These results may suggest a specific role of WINAC during embryogenesis, which may account for the diverse abnormalities in the WS patients.

Discussion

Purification and Identification of a Human Multiprotein Complex Containing WSTF, WINAC

WINAC contains known components of the hSWI/SNF-type complexes, including two major ATPase subunits, Brg1 and hBrm (Figure 2C). However, by our purification

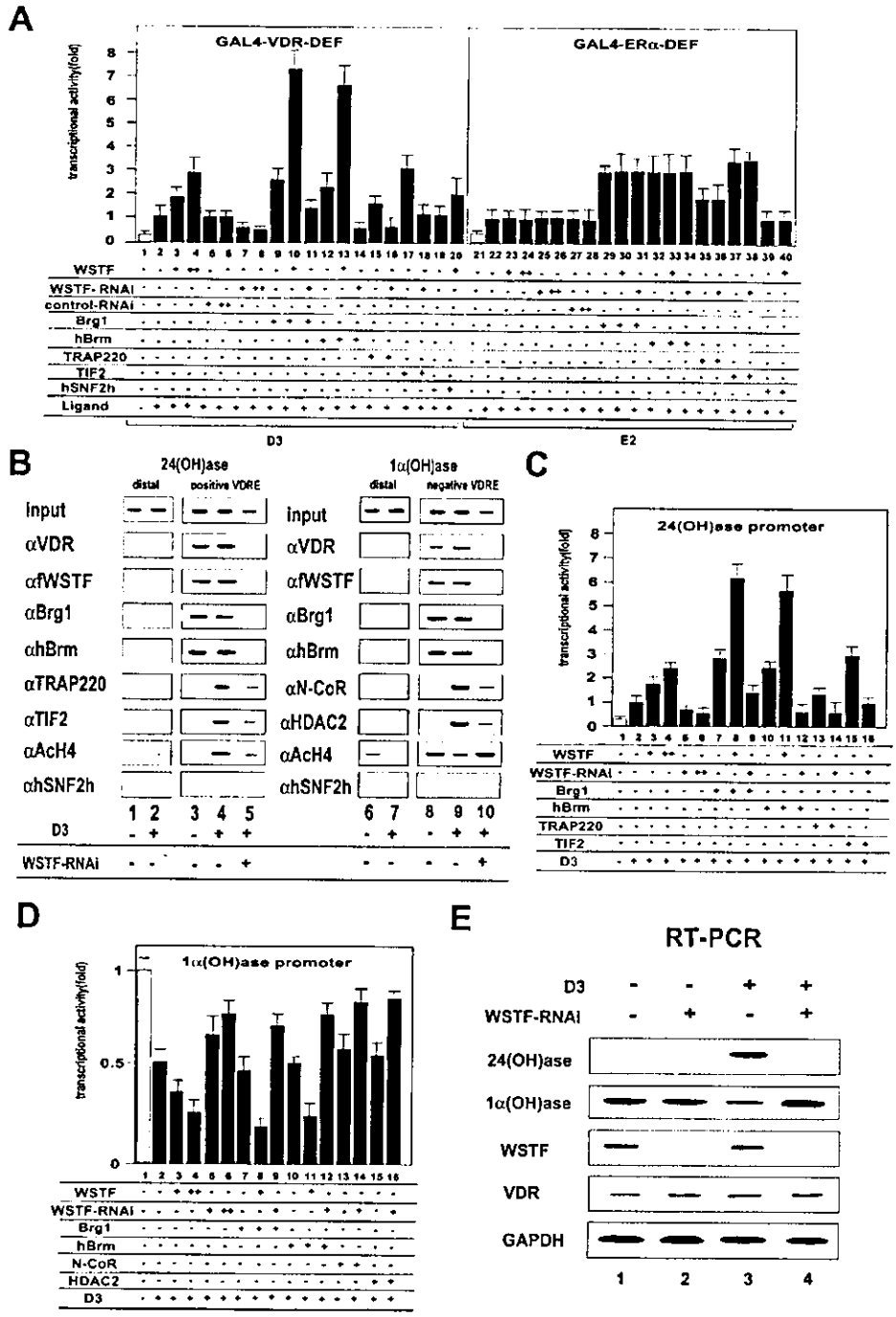

Figure 5. Ligand-Dependent Promoter Targeting of Coregulators through WINAC-VDR Association

(A) VDR-specific facilitation of co-activator accessibility by WINAC. MCF7 cells were transfected with the expression vectors of a luciferase reporter plasmid containing the GAL4 upstream activation sequence (UAS) [17mer(×2)] driven by the β-globin promoter (0.5 μg). PML-CMV (2 ng); GAL4-DBD-VDR-DEF (0.2 μg); GAL4-DBD-ERα DEF (0.2 μg); pDNA3-FLAG-WSTF (+; 0.1 μg: ++; 0.3 μg); pSV-Brg1 (0.2 μg); pSV-hBrm (0.2 μg); pcDNA3-TRAP220 (0.3 μg); pcDNA3-TIF2 (0.3 μg); siRNA (+; 0.1 μg: ++; 0.2 μg) of WSTF-RNAi; or control RNAi or their combinations were transfected as indicated in the images in the absence or presence of ligand (10^{-9} M). Bars in each graph show the fold change in luciferase activity relative to the activity of the receptor transactivation in the presence of ligand.

(B) ChIP analysis on the 24(OH)ase promoter and 1α(OH)ase promoter of WSTF stable transformants. Soluble chromatin was prepared from WSTF stable transformants treated with D3 (10^{-9} M) for 45 min and immunoprecipitated with indicated antibodies.

(C and D) The coregulator-like actions of WSTF on the naturally occurring positive and negative vitamin D response elements. MCF7 cells were transfected with the expression vectors of either the luciferase reporter plasmid containing a human 24(OH)ase promoter harboring a canonical positive VDRE or a human 1α(OH)ase promoter containing a negative VDRE and the factors shown in (A) or together with pcDNA3-N-CoR (0.3 μg), pcDNA3-HDAC2 (0.3 μg).

(E) WSTF-mediated regulations of endogenous genes by VDR. RT-PCR analysis of MCF7 cells was performed 12 hr after the induction by D3 (10^{-9} M) (Yanagisawa et al., 2002).

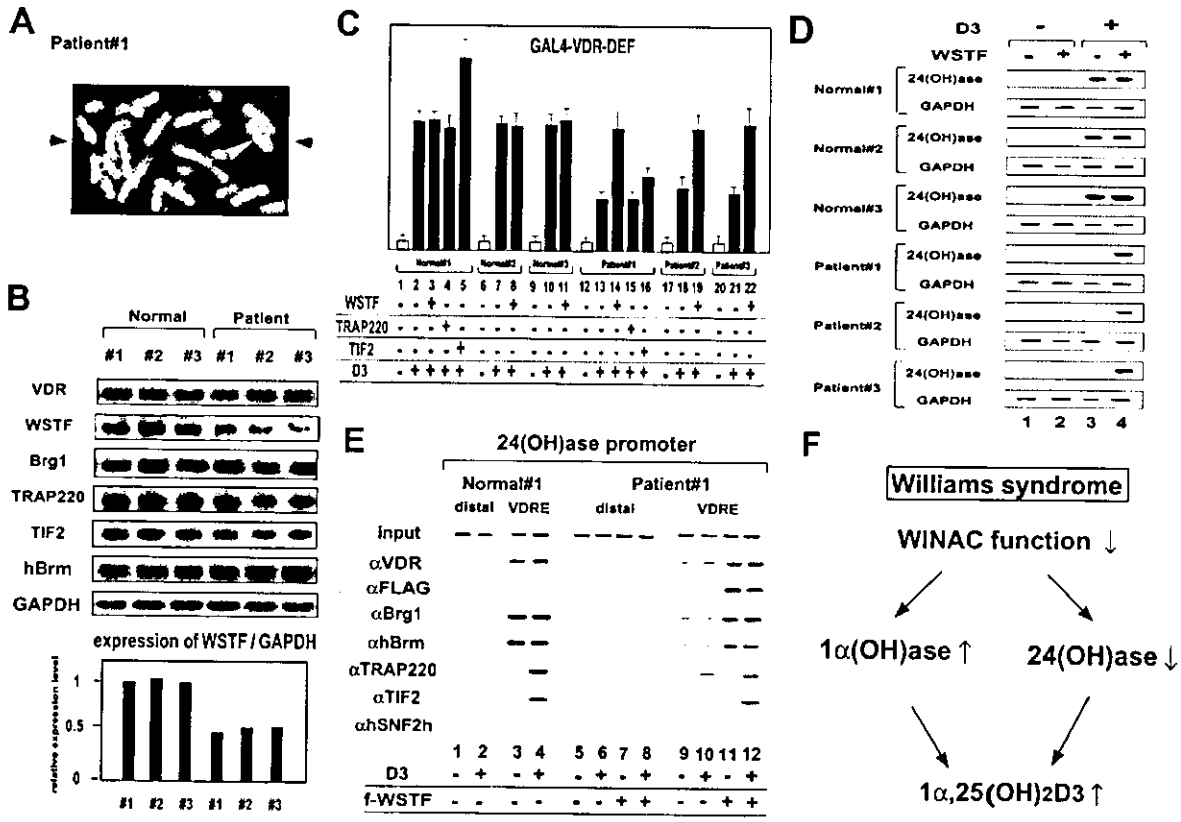

Figure 6. Impaired VDR Function in the Fibroblasts of Williams Syndrome Patients Was Recovered by WSTF Overexpression

(A) Fluorescence in situ hybridization of WS patient 1, confirming a deletion of one copy of the WSTF gene. The black arrowhead indicates D7S427 gene locus and the white arrowhead for WSTF gene. D7S427 was used for a chromosome 7 marker and cosmid full-length WSTF for WSTF gene probe.

(B) Reduced WSTF expression levels in WS skin fibroblasts. The indicated genes were examined for expression by Northern blotting with GAPDH expression as an internal control (Yanagisawa et al., 2002). Densitometric analysis of the relative expression level of WSTF versus GAPDH is shown in the lower image.

(C) VDR transactivation functions were impaired in the skin fibroblasts of the WS patients. Fibroblasts from controls and patients were transfected with the expression vectors as described in Figure 5A and the receptor function was tested.

(D) WSTF overexpression recovered the impaired responsiveness to vitamin D during 24(OH)ase gene induction. Patient's skin fibroblasts were transfected with an adenovirus expressing FLAG-WSTF, and treated with 1α,25(OH)2D3 (10^{-9} M) for 12 hr. Total RNA was subjected to RT-PCR analysis of 24(OH)ase expression.

(E) Impaired promoter targeting of VDR, coregulators, and WINAC components in fibroblasts from WS patients was rescued by WSTF overexpression. ChIP assays of the patient skin fibroblasts were performed with adenovirus expressing FLAG-WSTF as described in Figure 5B.

(F) Hypothesis of the cause of hypercalcemia in Williams syndrome patients.

methods we could detect neither the PBAF complex nor its specific component (BAF180). Moreover, by our purification, no ISWI-based complex was detectable even in the glycerol gradient fractions containing complexes with expected molecular weights. These observations are also different from a report that WSTF forms a hISWI-based chromatin-remodeling complex (Bozhenok et al., 2002). Confirming that hISWI (hSNF2h) expression did not affect the VDR transactivation function (Figures 5A and 5B), the combination with ISWI-based complex components looks to deter WSTF from the VDR interaction.

Of note, WINAC harbors three components, which have not yet been found in the ATP-dependent chromatin-remodeling complexes. Two factors (CAF-1p150 and TopoIIβ are integrated in the complexes serving roles in DNA replication (Smith and Stillman, 1989; Varga-Weisz et al., 1997), while FACT p140 is involved in a complex that promotes chromatin-dependent transcriptional elongation with an ISWI-type complex (LeRoy et al., 1998). From the observed WSTF interactions with the other subunits in vitro (Figures 3A–3D), WSTF appears to serve as a core protein to form an SWI2/SNF2-based complex, generating a subclass of the ATP-dependent chromatin-remodeling complex with DNA replication-related factors. Taken together, WSTF may serve as a dual platform protein capable of forming both SWI/SNF- and ISWI-type chromatin-remodeling complexes by distinct subunit combinations, but only the SWI/SNF-type WINAC selectively assists VDR function through a physical interaction.

WINAC Is a Chromatin-Remodeling Complex

Specific and more efficient targeting of VDR through WINAC to the VDREs was supported from functional analyses of the purified WINAC in vitro. In this respect,

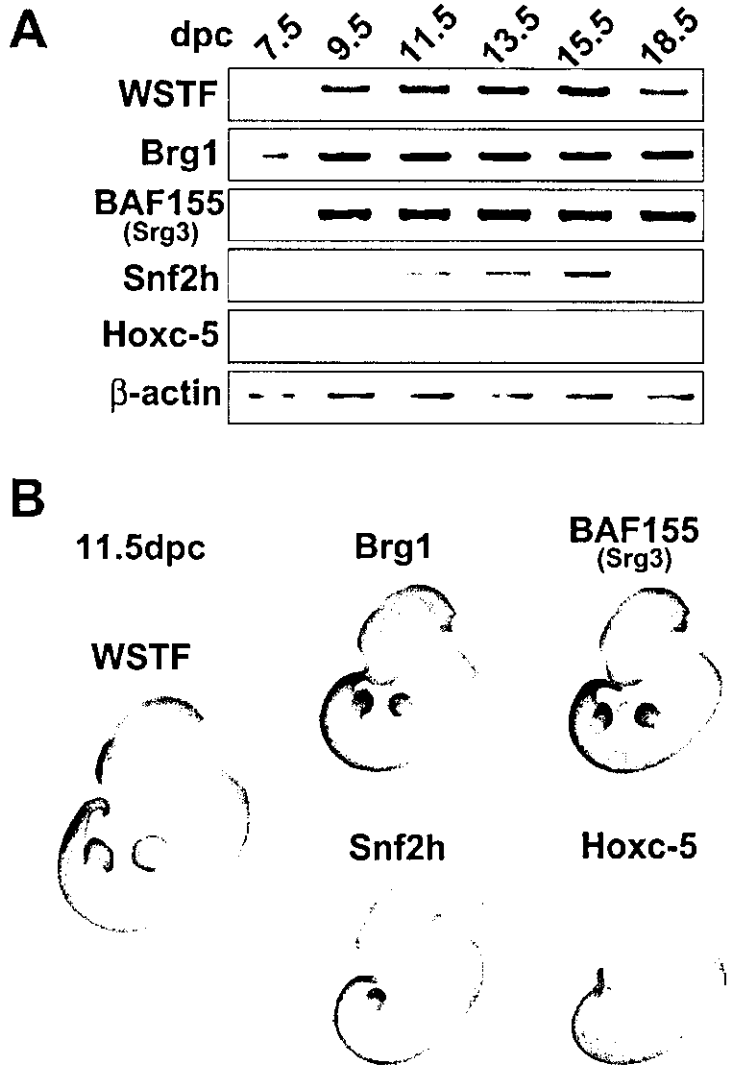

Figure 7. Spatiotemporal Expression Patterns of WSTF during Mouse Embryogenesis

(A) RT-PCR analysis of mouse WSTF, Brg1, BAF155 (Srg3), Snf2h, Hoxc-5, and β-actin gene expression. Embryos were dissected at the indicated times (7.5 dpc to 18.5 dpc). Samples were normalized by dilution to give equivalent signals for β-actin.

(B) Whole mount in situ hybridization analysis of mouse WSTF, Brg1, BAF155 (Srg3), Snf2h, and Hoxc-5 (negative control) expression at 11.5 dpc (Scale bar: 2 mm. Sense control probes were also hybridized and no signal was detected; data not shown).

WINAC subunit configuration is of interest to be clarified for defining the function of each component. A recent report has revealed that the chromatin-remodeling activity of the dISWI-based complex requires multiple Acf1 motifs to nonspecifically anchor DNA through its WAC motifs, and to directly interact with ISWI through the DDT domain (Fyodorov and Kadonaga, 2002). In addition to a core subunit role of WSTF, multiple functions as a pivotal factor to conduct the WINAC function could be further speculated from the conservation of several motifs that are shared with the other WAC family proteins, like hACF1 (Jones et al., 2000). Moreover, functions of the bromodomain and PHD finger motif in WSTF remain to be established in the promoter targeting and chromatin remodeling (Hassan et al., 2002; Schultz et al., 2002).

Promoter Targeting of VDR by WINAC and Cooperative WINAC Function with the Coregulator Complexes

Similar to the reported coactivator-like actions of the SWI2/SNF2 ATPases and BAF57 for the ligand-induced ERα transactivation (Chiba et al., 1994; DiRenzo et al., 2000; Belandia et al., 2002), overexpression of WSTF and the ATPase subunits as well could coactivate the ligand-induced VDR transactivation as either a GAL4 DBD chimeric protein or heterodimer with RXR (Figures 5A and 5C). VDR coactivation by the ligand-dependent NR coactivators (TIF2 and TRAP220) was abrogated by WSTF-RNAi expression (Figure 5A). However, neither such coactivator-like WSTF actions nor reduced coactivation by NR coactivators by the WSTF-RNAi expression was detected for ERα (Figure 5A) and the other receptors tested (data not shown), supporting the observed direct and selective interaction of WSTF with VDR among NRs (Figure 1D). Moreover, WSTF overexpression potentiated the ligand-induced transrepression of VDR on the 1α(OH)ase negative VDRE (Figure 5D), where an ablation of endogenous WSTF by RNAi expression led to a significant reduction in ligand-induced corepressor recruitment (lane 10 in Figure 5B). Thus, ligand-independent association of WINAC and VDR in the VDR target promoters appears to facilitate the local nucleosomal array

accessibility for ligand-dependent coregulators, following histone tail modifications by the recruited coregulator complexes (Hassan et al., 2002). It was recently reported that only when ligand is bound to ERα, all of the ERα p160/CBP HAT coactivator complex and human SWI/SNF-type complexes are targeted to the ER target promoters, although such ligand-induced occupancy of ERα and coregulator in the promoters appears in a cyclic fashion (Shang et al., 2000; Belandia et al., 2002). Such ligand-induced assembly of the SWI/SNF-type complexes with NRs through the p160/CBP complex might be a common mechanism for ligand-dependent targeting of NRs to the cognate promoters (Glass and Rosenfeld, 2000).

Unlike NRs such as ERα and AR (Belandia et al., 2002; Shang et al., 2002), VDR appears from ChIP analysis (Figure 5B) to be selectively targeted through WINAC to the promoters without ligand-induced activation of VDR function or following recruitment of coregulator complexes. WINAC targeting to the promoters appears not to require specific histone tail modifications by coregulators. Thus, it is likely that WINAC associating on promoters escort VDR for its recognition and specific binding to VDREs, through nucleosomal mobilization by WINAC, presumably cooperating with the other chromatin complexes (Lemon et al., 2001). Alternatively, once VDR happens to bind VDREs during nonspecific chromatin remodeling, WINAC might be acquired to VDR upon the promoters to engage in local nucleosome reorganization. The latter possibility coincides well with a recent report about a sequence-specific regulator, SATB1 (Yasui et al., 2002). As a result, the local chromatin structure near VDREs may transit into an active chromosomal state that appears competent for receipt of both the coactivator complexes and the corepressor complexes (Figures 5C and 5D) dependent on the VDRE sequences and the tertiary positions of DNA-bound VDR. This is not consistent with recent observations that the chromatin-remodeling complexes are recruited only after acetylation/deacetylation of histone tails by the coregulatory complexes (Hassan et al., 2002). However, the orders of the complex targetings are supposed to be dependent on the regulator type and the promoter context (Lomvardas and Thanos, 2002; Soutoglou and Talianidis, 2002).

Williams Syndrome Is a Chromatin-Remodeling Factor Disease?

We found that the ligand-induced transactivation function of VDR is impaired in the skin fibroblast cells of all three tested patients, in whom the regions covering the WSTF gene locus at the chromosome 7q11.23 are heterozygously deleted. Such impaired VDR function should not lead to severe defects in vitamin D actions in adults, since the adult VDR heterozygote mice ($VDR^{+/-}$) and the heterozygous carrier patients of the hereditary vitamin D-dependent type II rickets caused by VDR inactivation exhibited no overt abnormality in calcium and vitamin D metabolism, though VDR is a major regulator in those metabolisms (Yoshizawa et al., 1997). However, during growth, the mineral intakes must be greater than their excretions through the actions of calciotropic hormones, including vitamin D. It is tempting to speculate that the significantly reduced WINAC levels in WS patients transiently cause impaired function in VDR and other unidentified factors, leading to the transient appearance of infantile aberrant vitamin D metabolism and consequently, hypercalcemia (Taylor et al., 1982; Garabedian et al., 1985). These findings together suggest that a normal WSTF dose in the cells is necessary to support normal activities of VDR and presumably of some other regulators.

WSTF expression patterns during mouse embryogenesis overlap with those of the common components of WINAC (Bultman et al., 2000; Kim et al., 2001), but appear more limited. In contrast, the more restricted expression pattern was detected in mouse ISWI (Snf2h) (Lazzaro and Picketts, 2001) (Figure 7B). It is therefore possible to suggest that specific roles of WINAC among the other chromatin-remodeling complexes exert in a more spatiotemporal manner and support organogenesis of several selected tissues during embryogenesis through chromatin remodeling for, at least, transcription and DNA replication. Therefore, the WS patients may suffer a wide spectrum of disorders in certain organs. Thus, this study suggests that the Williams syndrome disorders are caused, at least in part, by WINAC dysfunction as a chromatin-remodeling disease.

Experimental Procedures

Plasmids and Antibodies

Chimeric GST proteins of GAL4 DBD (1–147 aa) fused with Rat VDR-DEF and WSTF deletion mutants were expressed in pGEX-2TK (Pharmacia Biotech). The promoter region of 1α,25-dihydroxyvitamin D3 24-hydroxylase (−367 to 0) and 25-hydroxyvitamin D3 1α-hydroxylase (−889 to −30) were inserted into the pGL3 vector (Promega) driven by a thymidine kinase (tk) promoter (Chen and DeLuca, 1995; Murayama et al., 1998; Yanagisawa et al., 2002). Rabbit polyclonal antipeptide antiserum was prepared by Sawady technology against KLQSEDSAKTEEVDEEKK, which is near the human WSTF C terminus.

Purification and Separation of VDR-Associated Complexes

For WINAC purification, the nuclear extracts of the MCF7 stable transformant were prepared by the same method as HeLa nuclear extracts (Rachez et al., 1998; Kitagawa et al., 2002; Yanagisawa et al., 2002). Then, they were bound to the GST column [GST], and 1α,25(OH)2D3-unbound GST-VDR column [GST-VDR(D3-)]. The complexes bound to the ligand-unbound VDR were eluted with 15 mM reduced glutathione in elution buffer (50 mM Tris-HCl [pH 8.3], 150 mM KCl, 0.5 mM EDTA, 0.5 mM PMSF, 5 mM NaF, 0.08% NP-40, 0.5 mg/ml BSA, and 10% glycerol). Next, they were layered on top of a 4.5 ml linear 100%–40% glycerol gradient in the GST binding buffer and centrifuged for 16 hr at 4°C at 40,000 rpm in a SW40 rotor (Beckman). Protein standards were ovalbumin (44 kDa), β-globulin (158 kDa), and thyroglobulin (667 kDa). Finally, the fractions containing WSTF and VDR were collected and loaded onto a 2.5–5 ml anti-FLAG M2 resin column (Sigma). After washing with binding buffer, the bound proteins were eluted by incubation for 60 min with 10–15 ml of the FLAG peptide (0.2 mg/ml) (Sigma) in binding buffer.

In Vitro Chromatin Reconstitution and Disruption Assay

Chromatin reconstitution and disruption reactions were performed essentially as previously described (Ito et al., 2000) using supercoiled plasmid DNA. A standard reaction contained plasmid (0.4 μg), purified core histones from *Drosophila* embryos (0.33 μg), purified recombinant dNAP1 (2.8 μg) [dNAP1], purified recombinant ACF (40 ng) [dACF], purified WINAC (100 ng) [WINAC], ATP (3 mM), and the ATP-regenerating system (30 mM phosphocreatine and 1mg/ml creatine phosphokinase). For the chromatin-disruption assay,

chromatin was reconstituted with DNA, pGIE0 (containing the GAL4 binding site) and purified histones by salt dialysis, and GST-GAL4 fusion proteins [e.g., GAL-VDR] mediated disruption of nucleosome arrays was analyzed by micrococcal nuclease digestion-Southern blot analysis.

In Vitro Transcription Assay

The purified proteins were purified as described previously (Ito et al., 2000). An in vitro transcription reactions and primer extension analysis was performed with pGI0 as an internal control, as previously described (Ito et al., 1997). Chromatin was reconstituted with DNA, pGIE0 (0.2 μg), and purified histones (0.24 μg) by salt dialysis and indicated purified GST-GAL4 fusion proteins (50 nM each final concentration), purified WINAC (50 ng) [WINAC] and p300 (40 nM) [p300] were added before the transcription reactions. After primer extension reactions, ^{32}P-labeled DNA was extracted by phenol-chroroform, precipitated by ethanol, analyzed on 8% acrylamide 8.3 M urea gels, and visualized by autoradiography.

In Vitro Replication Assay

An in vitro replication assay was performed as previously described (Ohba et al., 1996). Purified WINAC [WINAC], purified recombinant *Drosophila* NAP-1 [dNAP1], or *Drosophila* CAF-1[dCAF1] was added before initiating the DNA replication reactions. The products were extracted and subjected to electrophoresis in a 1.5% agarose gel (1 × TBE) and visualized by autoradiography.

Cell Cycle Analysis Using RNAi and DNA Quantity Analysis

For immunoprecipitation during the double-thymidine treatment, about 80% of the confluent cells of FLAG-WSTF stable transformants were treated with thymidine (2.5 mM). After 24 hr, the cells were washed and cultured in normal medium for 10 hr (first release), then were treated with hydroxyurea (1 mM), and cultured for 16 hr (Fujita et al., 1996). Finally, the cells were washed and cultured in normal conditions (final release), then immunoprecipitated with anti-FLAG M2-resin. For the analysis of the DNA histogram, the FACS analysis was done using FACS Calibur (BD PharMingen) and CellQuest (BD PharMingen) (Fujita et al., 1996).

RNAi Experiments

The two short RNAs were transfected after they were annealed. The sequence of the indicated RNAi is as follows: WSTF-RNAi (5′-GAGUAUGAAGCCCGCUUGGTT-3′ and 5′-CCAAGCGGGCUUCAUAC-UCTT-3′); Brg1-RNAi (5′-CUCCUCGGCCAGGUCCUUCTT-3′ and 5′-GAA-GGACCUGGCCGAGGAGTT-3′); Brm-RNAi (5′-UUCUUGGGCCUAGUC-CAGGTT-3′ and 5′-CCUGGACUAGGCCCAAGAATT-3′); CAF-1 p150-RNAi (5′-UCUUGUCCCAAA-GGGGAAATT-3′ and 5′-UUUCCCCUUUGG-GACAAGATT-3′); and control-RNAi (5′-CAGUAAGUAGCCGGGAUGGTT-3′ and 5′-CCAUCCCGGCUACUUA-CUGTT-3′).

ChIP Assay

Preparation of soluble chromatin for PCR amplification was performed as previously reported (Shang et al., 2000; Yanagisawa et al., 2002). The primer pairs for 24(OH)ase were 5′-GGGAGGCGCGTTCGAA-3′ and 5′-TCCTATGCCCAG-GGAC-3′ (pVDRE) and 5′-CCTCCTTTGCACAAGG-TAGT-3′ and 5′-AATGCACGTAAAGCGGCA-AC-3′ (distal); the primers for 1a(OH)ase were 5′-ATTCCCATGTCTGGAAGGAG-3′ and 5′-CAGTGAGC-CCAGCCCCTTTA-3′ (nVDRE) and 5′-AAGCTTGTCTCAACCTCCTG-3′ and 5′-GTTCAGAGATTGTCTGTGGG-3′ (distal).

Acknowledgments

We thank Dr. Michael Jones for kindly providing the partial WSTF cDNAs; Dr. H. Kato and Dr. H. Iba for Brg1 and hBrm plasmids; Dr. J. Kadonaga for dNAP-1; Dr. C. Wu for dACF; Dr. J.K. Tyler for dCAF-1; and Drs. G. Mizuguchi and L. Freedman for technical discussion. We also thank Dr. K. Yamane, H. Kawano, and A. Unno for the technical support; Dr. L. Tora for the critical discussion; and Miss H. Higuchi for preparation of the manuscript. This work was supported in part by a grant-in-aid for priority areas from the Ministry of Education, Science, Sports, and Culture of Japan (S.K.).

Received: December 30, 2002
Revised: May 16, 2003
Accepted: May 28, 2003
Published: June 26, 2003

References

Belandia, B., Orford, R.L., Hurst, H.C., and Parker, M.G. (2002). Targeting of SWI/SNF chromatin remodelling complexes to estrogen-responsive genes. EMBO J. *21*, 4094–4103.

Bozhenok, L., Wade, P.A., and Varga-Weisz, P. (2002). WSTF-ISWI chromatin remodeling complex targets heterochromatic replication foci. EMBO J. *21*, 2231–2241.

Bultman, S., Gebuhr, T., Yee, D., La Mantia, C., Nicholson, J., Gilliam, A., Randazzo, F., Metzger, D., Chambon, P., Crabtree, G., and Magnuson, T. (2000). A Brg1 null mutation in the mouse reveals functional differences among mammalian SWI/SNF complexes. Mol. Cell *6*, 1287–1295.

Chen, K.S., and DeLuca, H.F. (1995). Cloning of the human 1 alpha,25-dihydroxyvitamin D-3 24-hydroxylase gene promoter and identification of two vitamin D-responsive elements. Biochim. Biophys. Acta *1263*, 1–9.

Chiba, H., Muramatsu, M., Nomoto, A., and Kato, H. (1994). Two human homologues of Saccharomyces cerevisiae SWI2/SNF2 and Drosophila brahma are transcriptional coactivators cooperating with the estrogen receptor and the retinoic acid receptor. Nucleic Acids Res. *22*, 1815–1820.

DiRenzo, J., Shang, Y., Phelan, M., Sif, S., Myers, M., Kingston, R., and Brown, M. (2000). BRG-1 is recruited to estrogen-responsive promoters and cooperates with factors involved in histone acetylation. Mol. Cell. Biol. *20*, 7541–7549.

Elbashir, S.M., Harborth, J., Lendeckel, W., Yalcin, A., Weber, K., and Tuschl, T. (2001). Duplexes of 21-nucleotide RNAs mediate RNA interference in cultured mammalian cells. Nature *411*, 494–498.

Emerson, B.M. (2002). Specificity of gene regulation. Cell *109*, 267–270.

Fujita, M., Kiyono, T., Hayashi, Y., and Ishibashi, M. (1996). hCDC47, a human member of the MCM family. Dissociation of the nucleus-bound form during S phase. J. Biol. Chem. *271*, 4349–4354.

Fyodorov, D.V., and Kadonaga, J.T. (2001). The many faces of chromatin remodeling: SWItching beyond transcription. Cell *106*, 523–525.

Fyodorov, D.V., and Kadonaga, J.T. (2002). Binding of Acf1 to DNA involves a WAC motif and is important for ACF-mediated chromatin assembly. Mol. Cell. Biol. *22*, 6344–6353.

Garabedian, M., Jacqz, E., Guillozo, H., Grimberg, R., Guillot, M., Gagnadoux, M.F., Broyer, M., Lenoir, G., and Balsan, S. (1985). Elevated plasma 1,25-dihydroxyvitamin D concentrations in infants with hypercalcemia and an elfin facies. N. Engl. J. Med. *312*, 948–952.

Glass, C.K., and Rosenfeld, M.G. (2000). The coregulator exchange in transcriptional functions of nuclear receptors. Genes Dev. *14*, 121–141.

Gu, W., Malik, S., Ito, M., Yuan, C.X., Fondell, J.D., Zhang, X., Martinez, E., Qin, J., and Roeder, R.G. (1999). A novel human SRB/MED-containing cofactor complex, SMCC, involved in transcription regulation. Mol. Cell *3*, 97–108.

Hassan, A.H., Prochasson, P., Neely, K.E., Galasinski, S.C., Chandy, M., Carrozza, M.J., and Workman, J.L. (2002). Function and selectivity of bromodomains in anchoring chromatin-modifying complexes to promoter nucleosomes. Cell *111*, 369–379.

Hoogenraad, C.C., Koekkoek, B., Akhmanova, A., Krugers, H., Dortland, B., Miedema, M., van Alphen, A., Kistler, W.M., Jaegle, M., Koutsourakis, M., et al. (2002). Targeted mutation of Cyln2 in the Williams syndrome critical region links CLIP-115 haploinsufficiency to neurodevelopmental abnormalities in mice. Nat. Genet. *32*, 116–127.

Ito, T., Bulger, M., Pazin, M.J., Kobayashi, R., and Kadonaga, J.T. (1997). ACF, an ISWI-containing and ATP-utilizing chromatin assembly and remodeling factor. Cell *90*, 145–155.

Ito, T., Ikehara, T., Nakagawa, T., Kraus, W.L., and Muramatsu, M. (2000). p300-mediated acetylation facilitates the transfer of histone H2A–H2B dimers from nucleosomes to a histone chaperone. Genes Dev. *14*, 1899–1907.

Jones, M.H., Hamana, N., Nezu, J., and Shimane, M. (2000). A novel family of bromodomain genes. Genomics *63*, 40–45.

Kamei, Y., Xu, L., Heinzel, T., Torchia, J., Kurokawa, R., Gloss, B., Lin, S.C., Heyman, R.A., Rose, D.W., Glass, C.K., and Rosenfeld, M.G. (1996). A CBP integrator complex mediates transcriptional activation and AP-1 inhibition by nuclear receptors. Cell *85*, 403–414.

Kim, J.K., Huh, S.O., Choi, H., Lee, K.S., Shin, D., Lee, C., Nam, J.S., Kim, H., Chung, H., Lee, H.W., et al. (2001). Srg3, a mouse homolog of yeast SWI3, is essential for early embryogenesis and involved in brain development. Mol. Cell. Biol. *21*, 7787–7795.

Kitagawa, H., Yanagisawa, J., Fuse, H., Ogawa, S., Yogiashi, Y., Okuno, A., Nagasawa, H., Nakajima, T., Matsumoto, T., and Kato, S. (2002). Ligand-selective potentiation of rat mineralocorticoid receptor activation function 1 by a CBP-containing histone acetyltransferase complex. Mol. Cell. Biol. *22*, 3698–3706.

Lazzaro, M.A., and Picketts, D.J. (2001). Cloning and characterization of the murine imitation switch (ISWI) genes: differential expression patterns suggest distinct developmental roles for Snf2h and Snf2l. J. Neurochem. *77*, 1145–1156.

Lemon, B., Inouye, C., King, D.S., and Tjian, R. (2001). Selectivity of chromatin-remodelling cofactors for ligand-activated transcription. Nature *414*, 924–928.

LeRoy, G., Orphanides, G., Lane, W.S., and Reinberg, D. (1998). Requirement of RSF and FACT for transcription of chromatin templates in vitro. Science *282*, 1900–1904.

Lomvardas, S., and Thanos, D. (2002). Modifying gene expression programs by altering core promoter chromatin architecture. Cell *110*, 261–271.

Loyola, A., LeRoy, G., Wang, Y.H., and Reinberg, D. (2001). Reconstitution of recombinant chromatin establishes a requirement for histone-tail modifications during chromatin assembly and transcription. Genes Dev. *15*, 2837–2851.

Lu, X., Meng, X., Morris, C.A., and Keating, M.T. (1998). A novel human gene, WSTF, is deleted in Williams syndrome. Genomics *54*, 241–249.

Mangelsdorf, D.J., Thummel, C., Beato, M., Herrlich, P., Schutz, G., Umesono, K., Blumberg, B., Kastner, P., Mark, M., Chambon, P., et al. (1995). The nuclear receptor superfamily: the second decade. Cell *83*, 835–839.

Murayama, A., Takeyama, K., Kitanaka, S., Kodera, Y., Hosoya, T., and Kato, S. (1998). The promoter of the human 25-hydroxyvitamin D3 1 alpha-hydroxylase gene confers positive and negative responsiveness to PTH, calcitonin, and 1 alpha,25(OH)2D3. Biochem. Biophys. Res. Commun. *249*, 11–16.

Narlikar, G.J., Fan, H.Y., and Kingston, R.E. (2002). Cooperation between complexes that regulate chromatin structure and transcription. Cell *108*, 475–487.

Ohba, R., Matsumoto, K., and Ishimi, Y. (1996). Induction of DNA replication by transcription in the region upstream of the human c-myc gene in a model replication system. Mol. Cell. Biol. *16*, 5754–5763.

Onate, S.A., Tsai, S.Y., Tsai, M.J., and O'Malley, B.W. (1995). Sequence and characterization of a coactivator for the steroid hormone receptor superfamily. Science *270*, 1354–1357.

Peoples, R.J., Cisco, M.J., Kaplan, P., and Francke, U. (1998). Identification of the WBSCR9 gene, encoding a novel transcriptional regulator, in the Williams-Beuren syndrome deletion at 7q11.23. Cytogenet. Cell Genet. *82*, 238–246.

Poot, R.A., Dellaire, G., Hulsmann, B.B., Grimaldi, M.A., Corona, D.F., Becker, P.B., Bickmore, W.A., and Varga-Weisz, P.D. (2000). HuCHRAC, a human ISWI chromatin remodelling complex contains hACF1 and two novel histone-fold proteins. EMBO J. *19*, 3377–3387.

Rachez, C., Suldan, Z., Ward, J., Chang, C.P., Burakov, D., Erdjument-Bromage, H., Tempst, P., and Freedman, L.P. (1998). A novel protein complex that interacts with the vitamin D3 receptor in a ligand-dependent manner and enhances VDR transactivation in a cell-free system. Genes Dev. *12*, 1787–1800.

Schultz, D.C., Ayyanathan, K., Negorev, D., Maul, G.G., and Rauscher, F.J., 3rd. (2002). SETDB1: a novel KAP-1-associated histone H3, lysine 9-specific methyltransferase that contributes to HP1-mediated silencing of euchromatic genes by KRAB zinc-finger proteins. Genes Dev. *16*, 919–932.

Sekine, K., Ohuchi, H., Fujiwara, M., Yamasaki, M., Yoshizawa, T., Sato, T., Yagishita, N., Matsui, D., Koga, Y., Itoh, N., and Kato, S. (1999). Fgf10 is essential for limb and lung formation. Nat. Genet. *21*, 138–141.

Shang, Y., Hu, X., DiRenzo, J., Lazar, M.A., and Brown, M. (2000). Cofactor dynamics and sufficiency in estrogen receptor-regulated transcription. Cell *103*, 843–852.

Shang, Y., Myers, M., and Brown, M. (2002). Formation of the androgen receptor transcription complex. Mol. Cell *9*, 601–610.

Smith, S., and Stillman, B. (1989). Purification and characterization of CAF-I, a human cell factor required for chromatin assembly during DNA replication in vitro. Cell *58*, 15–25.

Soutoglou, E., and Talianidis, I. (2002). Coordination of PIC assembly and chromatin remodeling during differentiation-induced gene activation. Science *295*, 1901–1904.

Taylor, A.B., Stern, P.H., and Bell, N.H. (1982). Abnormal regulation of circulating 25-hydroxyvitamin D in the Williams syndrome. N. Engl. J. Med. *306*, 972–975.

Varga-Weisz, P.D., Wilm, M., Bonte, E., Dumas, K., Mann, M., and Becker, P.B. (1997). Chromatin-remodelling factor CHRAC contains the ATPases ISWI and topoisomerase II. Nature *388*, 598–602.

Yanagisawa, J., Kitagawa, H., Yanagida, M., Wada, O., Ogawa, S., Nakagomi, M., Oishi, H., Yamamoto, Y., Nagasawa, H., McMahon, S.B., et al. (2002). Nuclear receptor function requires a TFTC-type histone acetyl transferase complex. Mol. Cell *9*, 553–562.

Yasui, D., Miyano, M., Cai, S., Varga-Weisz, P., and Kohwi-Shigematsu, T. (2002). SATB1 targets chromatin remodelling to regulate genes over long distances. Nature *419*, 641–645.

Yoshizawa, T., Handa, Y., Uematsu, Y., Takeda, S., Sekine, K., Yoshihara, Y., Kawakami, T., Arioka, K., Sato, H., Uchiyama, Y., et al. (1997). Mice lacking the vitamin D receptor exhibit impaired bone formation, uterine hypoplasia and growth retardation after weaning. Nat. Genet. *16*, 391–396.

MOLECULAR AND CELLULAR BIOLOGY, June 2002, p. 3698–3706 Vol. 22, No. 11
0270-7306/02/$04.00+0 DOI: 10.1128/MCB.22.11.3698–3706.2002

Ligand-Selective Potentiation of Rat Mineralocorticoid Receptor Activation Function 1 by a CBP-Containing Histone Acetyltransferase Complex

Hirochika Kitagawa,[1,2] Junn Yanagisawa,[1,3] Hiroaki Fuse,[4] Satoko Ogawa,[1] Yoshiko Yogiashi,[1,3] Atsuro Okuno,[5] Hiromichi Nagasawa,[5] Toshihiro Nakajima,[6] Toshio Matsumoto,[2] and Shigeaki Kato[1,3]*

Institute of Molecular and Cellular Biosciences[1] and Department of Applied Biological Chemistry, Graduate School of Agricultural and Life Sciences,[5] University of Tokyo, Bunkyo-ku, and Pharmacological Research Department, Teikoku Hormone Manufacturing Company, Ltd.,[4] Tokyo, First Department of Internal Medicine, University of Tokushima School of Medicine, Tokushima,[2] CREST, Japan Science and Technology, Kawaguchi, Saitama,[3] and Institute of Medical Science, St. Marianna University School of Medicine, Miyamae-ku, Kawasaki,[6] Japan

Received 16 November 2001/Returned for modification 31 January 2002/Accepted 21 February 2002

The rat mineralocorticoid receptor (MR) has two activation functions in distinct regions of the A/B domain, designated activation function 1a (AF-1a; amino acids 1 to 169) and AF-1b (amino acids 451 to 600). Since the p160 family protein TIF2, a known component of the AF-2 coactivator complex, potentiates the transactivation function of AF-1b but not that of AF-1a, it is likely that some other, novel protein complex interacts with the AF-1a region. Therefore, we attempted to identify such coactivator complexes from HeLa nuclear extracts by biochemical purification using a glutathione *S*-transferase–MR AF-1a fusion protein. Purified AF-1a region-interacting proteins were found to contain RNA helicase A (RHA) and CBP. Further analysis showed that RHA interacted with the AF-1a region directly and then recruited a complex with histone acetyltransferase (HAT) activity that contained CBP. For full-length MR, aldosterone, but not hydrocortisone, was found to induce the binding of RHA/CBP complexes to the AF-1a region, as well as to allow the cooperative potentiation of MR transcriptional activity by RHA and CBP. In addition, a chromatin immunoprecipitation assay showed that aldosterone-bound MR, but not hydrocortisone-bound MR, recruited RHA/CBP complexes to native MR target gene promoters. Our results suggested that an altered conformation of the A/B region induced by aldosterone, but not hydrocortisone, might determine the accessibility of MR AF-1a to RHA/CBP complexes.

Mineralocorticoid receptor (MR) is a member of the steroid/thyroid hormone nuclear receptor superfamily and acts as a ligand-inducible transcription factor responsible for ion homeostasis by regulating ion channel expression in epithelial cells (1, 5, 11, 14). Recently, it was shown that MR participates in a wide range of biological functions in nonepithelial tissues, including the heart and brain (5, 17, 32). MR has two native ligands, aldosterone (mineralocorticoid) and hydrocortisone (glucocorticoid), both of which bind MR and induce its transactivational function (26). However, the ligands mediate distinct physiological actions via MR (10, 20, 21, 40, 58). While these different physiological actions may partially depend on the enzymatic activity of 11β-hydroxysteroid dehydrogenase type 2 (11βHSD2), which inactivates hydrocortisone (glucocorticoid) and results in the preferential activation of MR by aldosterone in target tissues (15), this does not explain the distinct physiological actions of the two hormones in nonepithelial cells, where 11βHSD is not present (13, 34).

Nuclear receptors have two functional domains in their N-terminal A/B and C-terminal E/F domains. While autonomous activation function 2 (AF-2) in the C-terminal E/F domain is ligand binding dependent (49), autonomous activation function 1 (AF-1) in the N-terminal A/B domain is constitutively active, and unliganded nuclear receptors are able to block the transactivational function of AF-1 (31). Compared with the well-conserved E/F domains, the A/B domains, which contain AF-1, display no regions that are highly conserved between different nuclear receptors. We have previously detected two transactivational functions in MR, AF-1a and AF-1b, in the N-terminal A/B domain (16). Although previous studies have suggested a possible role for the A/B domain in ligand-selective functions of MR (26, 61), the physiological role of the A/B domain at the molecular level remains unclear.

DNA binding activators, like nuclear receptors, require basic transcription factors and coactivators for RNA polymerase II-mediated gene activation. RNA helicase A (RHA) is reported to be one of the components of the RNA polymerase II holoenzyme complex (36) and is a member of the DExH family of ATPase/helicases (48). Recent studies have shown that RHA interacts directly with coactivators and activators such as CBP/p300, BRCA1 (breast cancer-specific tumor suppressor protein), and SMN (survival motor neuron) to stabilize complex formation (2, 36, 39). These studies indicated that RHA might be a common coactivator acting as a bridging factor between basal transcription factors and activators.

For the ligand-induced transactivation function of nuclear receptors, two classes of coactivator complexes for AF-2 have been identified so far (11, 19). One is a histone acetyltransferase (HAT) complex thought to contain CBP/p300, p160

* Corresponding author. Mailing address: Institute of Molecular and Cellular Bioscience, University of Tokyo, 1-1-1 Yayoi, Bunkyo-ku, Tokyo 113-0032, Japan. Phone: 81-3-5841-7891. Fax: 81-3-5841-8477. E-mail: uskato@mail.ecc.u-tokyo.ac.jp.

protein family members (SRC-1 [steroid receptor coactivator 1], TIF2 [transcriptional intermediate factor 2], AIB1 [amplified in breast and ovarian cancer protein 1]), and an RNA coactivator, SRA, along with other, unknown components (3, 30, 38, 50, 53). Histone acetylation by intrinsic HAT activity of complexes converts the nucleosome into a transcriptionally active state by facilitating the access of activators to DNA binding (37). The other AF-2 coactivator complex is the recently reported DRIP (vitamin D receptor-interacting protein)/TRAP (thyroid hormone receptor-associated protein) complex, which is composed of at least 12 proteins but has no HAT activity (23, 41, 42). Although these coactivator complexes are reported to interact directly with the A/B domains of some nuclear receptors (8, 25, 27, 54, 55), little is known regarding AF-1-specific coactivator complexes. For MR, our observations that AF-1b, but not AF-1a, activity was enhanced by p160-family proteins support the existence of novel coactivator complexes for AF-1a (16).

In this study we attempted to identify MR AF-1a-interacting complexes by biochemical purification and mass fingerprinting by matrix-assisted laser desorption ionization–time-of-flight mass spectrometry (MALDI-TOF MS). One of the purified AF-1a region-interacting protein complexes was found to contain RHA and CBP (referred to below as the RHA/CBP complex). The interaction between RHA/CBP complexes and AF-1a was mediated through direct binding of RHA to the AF-1a region of MR. The finding that RHA did not bind to any MR region except AF-1a supported our previous observation that RHA potentiated the transcriptional activity of AF-1a but not that of AF-1b. For full-length MR, recruitment of the RHA/CBP complex to the AF-1a region was induced by aldosterone rather than hydrocortisone, which suggested that binding of hydrocortisone to MR may make the MR AF-1a region inaccessible to the RHA/CBP complex. Our results also raised the possibility that the differences between the biological activities of aldosterone and hydrocortisone in target tissues may be due to the ligand-selective recruitment of RHA/CBP complexes to MR.

MATERIALS AND METHODS

Plasmids. Rat MR deletion mutants FLAG-MR, FLAG-AF-1a, FLAG-AF-1b, FLAG-AF-2, and pcDNA-TIF2 were constructed as previously described (16). A series of rat MR deletion fragments (consisting of amino acids 1 to 169, 170 to 450, or 451 to 600, or fragment DEF) were inserted in-frame into the pAcG 2T vector (Pharmingen), while the series of RHA deletion mutants (with amino acids 1 to 262, 255 to 664, 649 to 1077, or 1064 to 1270 deleted) and the resultant chimeric proteins fused to glutathione *S*-transferase (GST) were as described previously (12). MREx2-tk-Luc was constructed by inserting two mineralocorticoid-responsive elements (MREs) from the tyrosine aminotransferase gene promoter into the pGL3-Basic vector (Promega) with a thymidine kinase (TK) promoter which was described previously (52, 54). Human CBP cDNA was obtained as several fragments by PCR using HeLa cell cDNA as the template and was reconstructed into pcDNA3, as described previously (36).

Antibodies. Antibodies used were an anti-FLAG M2 monoclonal antibody (F3165; Sigma), an anti-hemagglutinin (anti-HA) antibody (no. 561; Medical and Biological Laboratories Co., Ltd.), an anti-CBP antibody (sc369; Santa Cruz Biotechnology), an anti-MR antibody (sc11412; Santa Cruz Biotechnology), and an anti-RHA antibody (as previously described [36]).

Purification and separation of MR AF1a-interacting proteins. HeLa nuclear extracts were loaded onto a P11 phosphocellulose column. After extensive washes with washing buffer (20 mM Tris-HCl [pH 7.9], 150 mM KCl, 0.2 mM EDTA, 0.05% NP-40, 10% glycerol, 0.5 mM phenylmethylsulfonyl fluoride [PMSF], 1 mM dithiothreitol [DTT]), bound proteins were eluted by using elution buffer (20 mM Tris-HCl [pH 7.9], 1 M KCl, 0.2 mM EDTA, 0.05% NP-40, 10% glycerol, 0.5 mM PMSF, 1 mM DTT) and were then dialyzed in GST-binding buffer (20 mM Tris-HCl [pH 7.9], 180 mM KCl, 0.2 mM EDTA, 0.05% NP-40, 0.5 mM PMSF, 1 mM DTT) containing bovine serum albumin (1 mg/ml). After 4 to 5 h of dialysis, immobilized GST-MR AF-1a fusion proteins on the beads were incubated at 4°C for 6 to 10 h with HeLa nuclear extracts. After three washes with GST wash buffer (GST-binding buffer with 0.1% NP-40), the beads were further washed with GST wash buffer containing 0.2% *N*-lauryl sarcosine (Sarkosyl; Sigma). Complexes bound to MR AF-1a were eluted with 15 mM reduced glutathione in elution buffer (50 mM Tris-HCl [pH 8.3], 150 mM KCl, 0.5 mM EDTA, 0.5 mM PMSF, 5 mM NaF, 0.08% NP-40, 0.5 mg of bovine serum albumin/ml, and 10% glycerol). Eluates were then layered on top of a 4.5-ml linear 10-to-40% glycerol gradient in GST-binding buffer and centrifuged for 16 h at 4°C at 40,000 rpm in an SW40 rotor (Beckman). Each fraction (600 μl) was then applied to a Western blot using anti-CBP or anti-RHA antibodies. Protein standards used were vitamin B_{12} (1.3 kDa), myoglobin (17 kDa), ovalbumin (44 kDa), β-globulin (158 kDa), and thyroglobulin (667 kDa) (42, 54).

HAT assay. HAT activity in the glycerol density gradient fractions was assayed essentially as described previously (6). Briefly, the separated fractions were incubated with or without 10 μg of calf thymus histones (type IIA; Sigma) and ^{3}H-labeled acetyl coenzyme A (acetyl-CoA) (4.7 Ci/mmol; Amersham) for 30 min at 30°C, spotted onto Whatman P-81 filters, and washed extensively with sodium carbonate buffer (pH 9.1). Radioactivity remaining on the filter was then quantitated by liquid scintillation counting.

Protein identification by MALDI-TOF MS. Protein bands in sodium dodecyl sulfate-polyacrylamide gel electrophoresis (SDS-PAGE) gels were excised and in-gel digested with trypsin according to published procedures (24, 43, 45). Eluted peptides were then prepared on the sampling plate for MALDI-TOF MS (Voyager DE-STR; Perseptive Biosystems). After analysis of each protein fragment mass, results were compared by using the MS-Fit program (University of California—San Francisco Mass Spectrometry Facility).

GST pulldown assay. A series of MR and RHA deletion mutants fused to GST were expressed in a baculovirus and in *Escherichia coli*, respectively, as described elsewhere (4). The predicted sizes of the expressed proteins were verified by SDS-PAGE. For GST pulldown assays, baculovirus- and bacterially expressed GST fusion proteins or GST bound to glutathione-Sepharose 4B beads (Amersham Pharmacia Biotech) was incubated at 30°C with [^{35}S]methionine-labeled proteins expressed by in vitro translation using the TNT coupled transcription-translation system (Promega). Baculovirus-expressed GST-MR-DEF was preincubated with aldosterone (10^{-6} M) for 15 min at room temperature. After 2 h of incubation, free proteins were removed by washing the beads with NET-N$^+$ buffer (150 mM NaCl, 1 mM EDTA, 20 mM Tris-HCl [pH 7.5], 0.5% NP-40, 1 mM PMSF, 1 mM DTT). Specifically bound proteins were eluted by boiling in SDS sample buffer and then analyzed by SDS-PAGE. After electrophoresis, radiolabeled proteins were visualized with an image analyzer (BAS1500; Fuji Film, Tokyo, Japan) (56).

Immunoprecipitation. After 293T cells were washed twice with ice-cold phosphate-buffered saline, the collected cells were resuspended in 1 ml of ice-cold lysis buffer (10 mM Tris-HCl [pH 4.7], 10 mM NaCl, 3 mM $MgCl_2$, 0.5% [vol/vol] NP-40) and incubated on ice for 30 min; then they were centrifuged again for 5 min at 500 × *g*. The sedimented nuclear fractions were resuspended in TNE buffer (10 mM Tris-HCl [pH 7.5], 1% NP-40, 0.15 M NaCl, 1 mM EDTA) and incubated for 30 min on ice. After centrifugation, supernatants were used as whole-cell extracts of 293T cells for immunoprecipitation using an anti-FLAG M2 affinity resin (no. A2220; Sigma) after Western blotting with anti-FLAG M2 monoclonal, anti-HA, or anti-CBP antibodies.

Chromatin immunoprecipitation (ChIP) assay. HEK293 cells were cultured for 3 to 4 days in media supplemented with 10% charcoal-dextran stripped serum and were then infected with rat MR and RHA adenovirus expression constructs made by using the Adeno-X Expression System (Clontech Laboratories Inc.). After 2 days, cultures were treated with aldosterone (10^{-8} M) or hydrocortisone (10^{-8} M) for 45 min and immunoprecipitated with specific antibodies for MR, RHA, or CBP. Soluble chromatin was prepared by using an acetyl-histone H4 immunoprecipitation assay kit (Upstate Biotechnology) and was immunoprecipitated with antibodies against the indicated proteins. Extracted DNA samples were amplified with primer pairs Na-K-ATPase α1 (5′-CAGATTCTCAT TTT GGAATCTCGAAG-3′ and 5′-GATCTCCTCTGGGACTCA-3′) and αENaC (5′-TTCCTTTCCAGCGCTGGCCAC-3′ and 5′-CCTCCAACCTTGT CCAGA CCC-3′). Optimized PCR conditions used to allow semiquantitative measurement were 20 cycles of 30 s at 96°C, 15 s at 56°C, and 1 min at 72°C. PCR products were visualized on 2% agarose–Tris-acetate EDTA gels.

Luciferase assay. 293T cells were transfected by using Lipofectin reagent (GIBCO BRL). A luciferase reporter plasmid containing two MREs and the thymidine kinase promoter (MREx2-tk-Luc) was cotransfected with expression

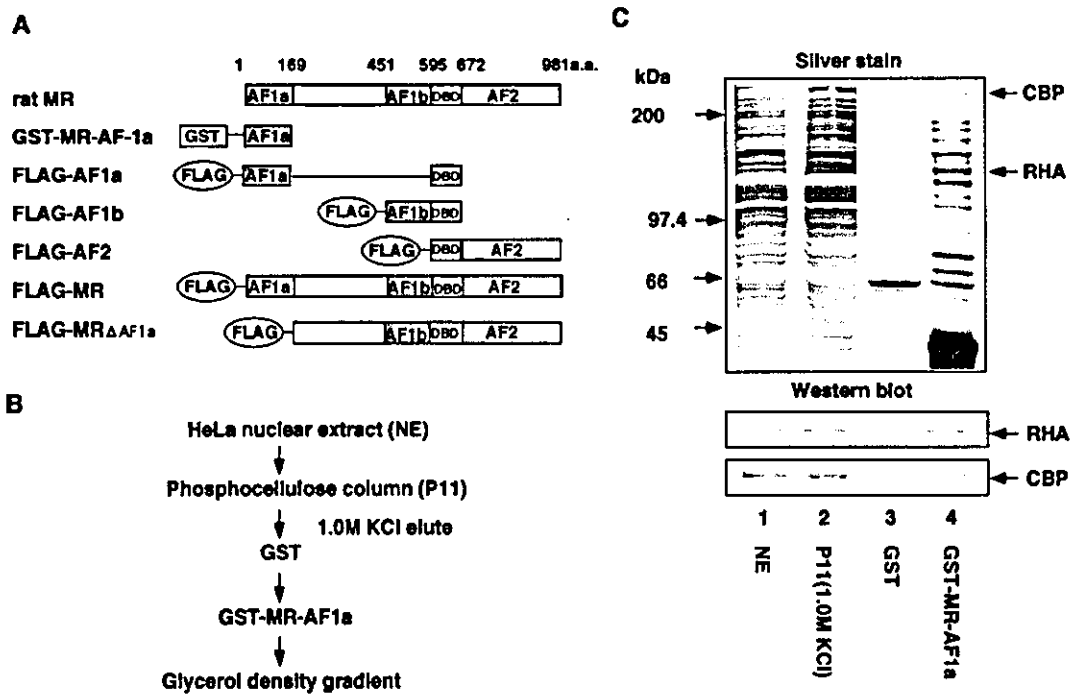

FIG. 1. Purification and identification of MR AF-1a-binding complexes. (A) Schematic representation of rat MR activation domains and deletion mutants. AF-1a and AF-1b are ligand-independent activation regions within the rat MR A/B domain. GST-fused MR AF-1a (GST-MR-AF-1a) was used as bait for binding-complex purification. A DNA binding domain (DBD) was present in all rat MR deletion mutants (FLAG-AF1a, FLAG-AF1b, FLAG-AF2, and FLAG-MRΔAF1a). (B) Purification scheme for MR AF-1a interactants. Nuclear extracts from HeLa S3 cells were applied to P11 phosphocellulose columns. After extensive washes with wash buffer (20 mM Tris-HCl [pH 7.9], 0.2 mM EDTA, 0.05% NP-40, 10% glycerol, 0.5 mM PMSF, 1 mM DTT) containing 0.15 M KCl, bound proteins were eluted with wash buffer containing 1.0 M KCl. Eluted fractions were then incubated with immobilized GST-MR-AF-1a, and MR AF1a-interacting proteins were eluted by using *N*-lauryl sarcosine. (C) Identification of MR AF-1a interactants. The indicated fractions were subjected to SDS-PAGE followed by silver staining. Total HeLa S3 nuclear extracts (NE) (lane 1), a fraction eluted from a P11 column (P11) (lane 2), and eluted fractions from GST and GST-MR-AF-1a (lanes 3 and 4) are shown. Proteins eluted from GST-MR-AF-1a (lane 4) were identified by MS analysis. Lower panels show Western blotting for each fraction using antibodies against RHA or CBP.

vectors as indicated in the figure legends. Six hours after transfection, the medium was replaced with fresh medium containing 0.2% fetal bovine serum. At this time, aldosterone (10^{-9} M) or hydrocortisone (10^{-9} M) ligands were added, and cells were incubated for an additional 12 h. Preparation of cell extracts and dual luciferase assays were performed according to the manufacturer's protocols (Promega). Individual transfections, each consisting of triplicate wells, were repeated at least three times.

RESULTS

A HAT complex containing RHA and CBP interacts with rat MR AF-1a. To identify coactivator complexes for rat MR AF-1a, HeLa cell nuclear extract fractions, prepurified on phosphocellulose columns, were incubated with either GST-fused AF-1a protein or GST protein alone. After extensive washing, bound proteins were eluted by reduced glutathione and subjected to SDS-PAGE analysis. Protein bands which specifically bound to GST-MR-AF-1a protein were subjected to peptide mass fingerprinting by MALDI-TOF MS. Obtained masses and apparent molecular weights of the different polypeptides revealed that the fraction eluted from the AF-1a fusion protein contained RHA and CBP. Mass fingerprinting results were confirmed by Western blotting using specific antibodies against RHA and CBP (Fig. 1C). The presence of CBP in the purified fraction was consistent with our previous findings that CBP/p300 enhanced AF-1a activity (16) and with another study in which interaction between CBP and RHA was observed (36). Thus, the AF-1a region may interact with a coactivator complex containing both CBP and RHA.

AF-1a region-interacting proteins were further fractionated according to molecular mass by using a glycerol density gradient. Since CBP has HAT activity, HAT activity for each fraction was assessed (Fig. 2B). Proteins in each fraction were separated by SDS-PAGE in parallel and were either silver stained or analyzed by Western blotting using specific antibodies against RHA and CBP (Fig. 2A and C, respectively). RHA and CBP were detected in fractions that possessed high HAT activity and were included in a multiprotein complex of more than 670 kDa, which suggested that a CBP-containing HAT multiprotein complex (designated the RHA/CBP complex) bound MR AF-1a (Fig. 2C).

RHA interacts directly with MR AF-1a. To test whether RHA and CBP interacted directly with the AF-1a region, a GST pulldown assay was performed by using a series of GST-fused MR and RHA deletion mutants, together with in vitro-translated proteins. While RHA directly bound the N-terminal region (amino acids 1 to 169) of MR, CBP did not bind to any of the MR A/B domain deletion mutants (Fig. 3A). We then

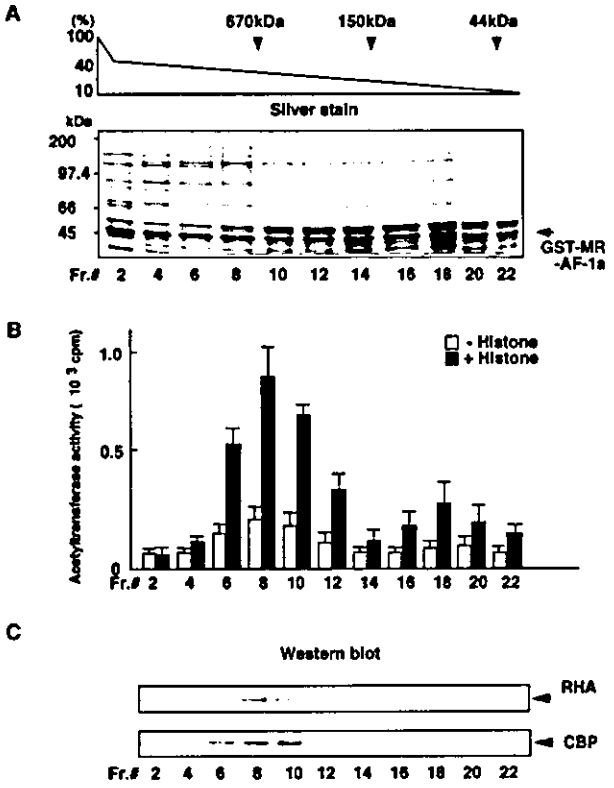

FIG. 2. A HAT complex containing RHA and CBP interacts with MR AF-1a. (A) Glycerol density gradient analysis. Fractions eluted on a P11 column were passed over an immobilized GST-MR-AF-1a column. Protein complexes bound to GST-MR-AF-1a were then dissociated by reduced glutathione and applied to 10-to-40% glycerol density gradients. Each fraction was subjected to SDS-PAGE followed by silver staining. The positions of marker proteins with known molecular masses on the gradient are indicated. (B) HAT activity in the glycerol density gradient fractions. The indicated fractions were incubated with or without free histones, together with ^{3}H-labeled acetyl-CoA, and assayed for HAT activity in a filter-binding assay as described in Materials and Methods. HAT activity is quantitated as counts per minute of ^{3}H-labeled acetate transferred from acetyl-CoA to histones. (C) Western blot analysis of glycerol density gradient fractions. To identify the proteins contained in each gradient fraction, Western blot analysis was performed with specific antibodies against RHA or CBP.

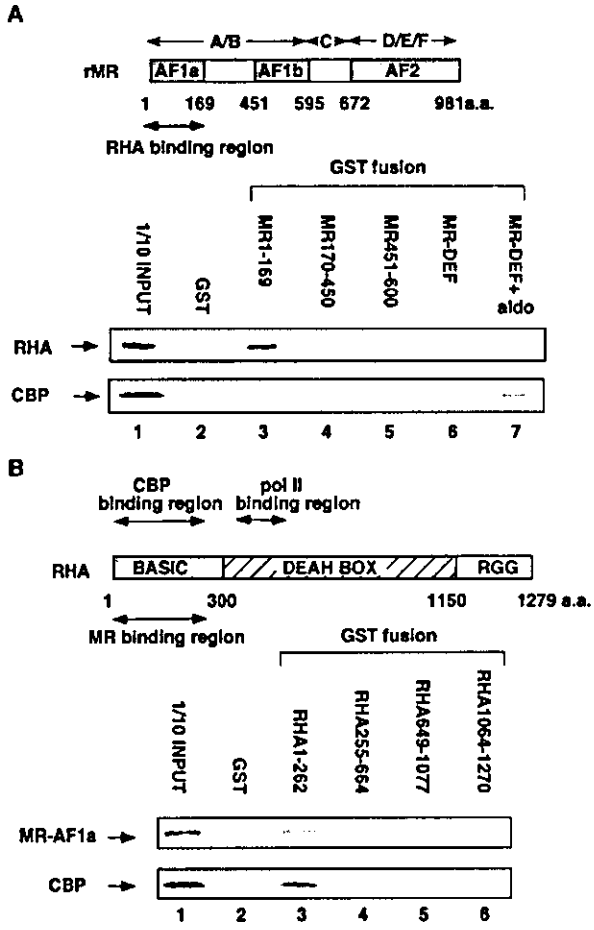

FIG. 3. RHA interacts directly with MR AF-1a. (A) RHA, but not CBP, interacts directly with MR AF-1a. A GST pulldown assay was performed as described in Materials and Methods. A series of MR deletion mutants fused to GST were expressed by a baculovirus, and the GST fusion proteins were immobilized on glutathione-Sepharose beads. In vitro-translated RHA and CBP were incubated with glutathione-Sepharose beads loaded with each MR mutant fused to GST (for GST-MR-DEF, in the absence and presence of 10^{-6} M aldosterone). Bound proteins were subjected to SDS-PAGE followed by autoradiography. rMR, rat MR; aldo, aldosterone. (B) Mapping of the MR binding region to the N-terminal domain of RHA. A series of RHA deletion mutants fused to GST were expressed by *E. coli* and immobilized on glutathione-Sepharose beads. In vitro-translated MR AF-1a and CBP were then incubated with the glutathione-Sepharose beads loaded with each RHA mutant fusion protein. Bound proteins were subjected to SDS-PAGE followed by autoradiography.

tested for interaction between RHA and AF-1a or CBP. The AF-1a region exhibited affinity for the N-terminal region (amino acids 1 to 262) of RHA (Fig. 3B). As expected from previous studies, we observed direct binding of CBP to the basic region of RHA (36). However, we failed with the N-terminal deletion mutants to map the core regions for the interactions, because RHA and CBP could not be distinguished in the interactions. The physical interactions appeared to require that the protein structures of the interacting regions be intact. These results suggested that RHA within the RHA/CBP complex acted as the interface for the AF-1a region.

RHA/CBP complexes are recruited to MR bound on the target gene promoters in the presence of aldosterone but not hydrocortisone. We then used coimmunoprecipitation to test whether interaction between AF-1a and RHA/CBP complexes took place in living cells. By use of antibodies against FLAG and HA, both HA-RHA fusion protein and endogenous CBP were detected by Western blotting in AF-1a immunoprecipitates from extracts of expression vector-transfected 293T cells. Increased amounts of CBP were immunoprecipitated with AF-1a in cells that overexpressed RHA (Fig. 4A, lane 4), which supported our finding that RHA mediated the indirect association of CBP with MR AF-1a. We next tested for in vivo interaction between full-length MR and RHA/CBP complexes. Like the AF-1a region, full-length MR also coimmunoprecipitated with CBP and RHA in an aldosterone-dependent manner, with increased CBP retention in immunoprecipitates from

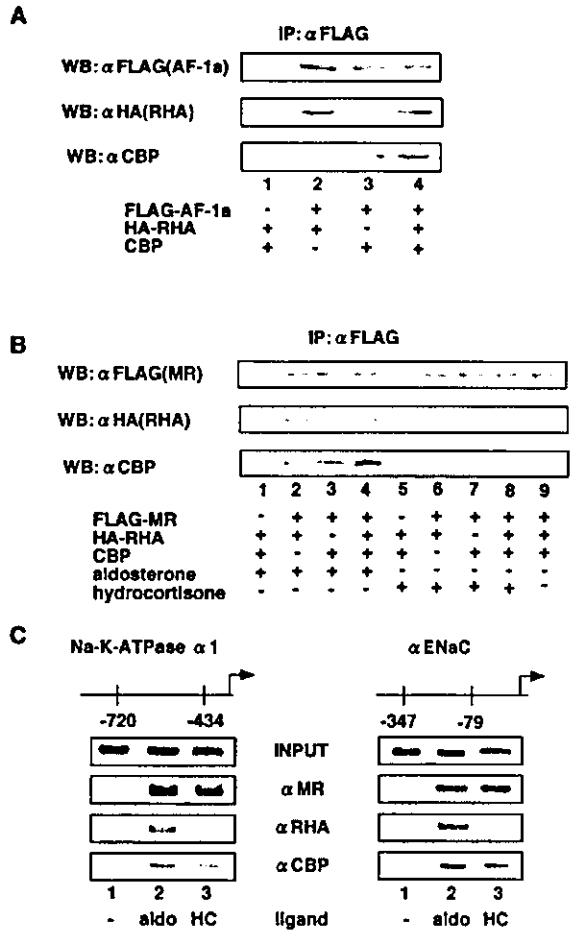

FIG. 4. Ligand-selective recruitment of RHA-CBP complexes to MR AF-1a in vivo. (A) RHA/CBP complexes interact with MR AF-1a in vivo. 293T cells were cotransfected with or without 5 μg of pc-DNA-FLAG-MR-AF-1a, pc-DNA-HA-RHA, or pc-DNA-CBP. Cells were lysed in TNE buffer and subjected to immunoprecipitation (IP) using an anti-FLAG (αFLAG) affinity resin. Precipitates were Western blotted by using antibodies against FLAG, HA, or CBP as indicated. (B) Aldosterone, but not hydrocortisone, induces interaction between RHA/CBP complexes and MR. 293T cells were cotransfected with or without 5 μg of pc-DNA-FLAG-MR, pc-DNA-HA-RHA, or pc-DNA-CBP in the presence or absence of 10^{-8} M aldosterone or hydrocortisone. Cells were lysed in TNE buffer and subjected to immunoprecipitation using an anti-FLAG affinity resin. Precipitates were Western blotted with antibodies against FLAG, HA, or CBP as indicated. (C) RHA/CBP complexes are recruited to the MR target gene promoters Na-K-ATPase α1 and αENaC in an aldosterone-dependent manner. HEK293 cells were transfected with an adenovirus expressing rat MR and RHA. Soluble chromatin was prepared from HEK293 cells treated with 10^{-8} M aldosterone (aldo) or hydrocortisone (HC) for 45 min and was immunoprecipitated with antibodies against MR, RHA, or CBP. (i.e., the ChIP assay was performed). DNA was then extracted and amplified with pairs of primers covering the Na-K-ATPase α1 and αENaC gene promoter regions as indicated.

RHA-overexpressing cells (Fig. 4B, lanes 1 to 4). However, in the presence of hydrocortisone, coimmunoprecipitation of MR and RHA was not detected and no increase in the level of MR-associated CBP was observed when RHA was overexpressed (Fig. 4B, lanes 5 to 8).

To further investigate whether the RHA/CBP complex was indeed recruited to MR in the presence of aldosterone rather than hydrocortisone in living cells, we performed a ChIP assay using promoters from the MR target genes encoding the Na-K-ATPase α1 subunit and the α subunit of the epithelial sodium channel (αENaC) (29, 35, 46). MR was recruited together with RHA/CBP complexes to the promoter regions of both target genes in the presence of aldosterone, but not in the presence of hydrocortisone, supporting the hypothesis that aldosterone selectively induced the recruitment of RHA/CBP complexes to MR (Fig. 4C).

RHA and CBP cooperatively enhance MR AF-1a transactivation. To test whether the aldosterone-induced recruitment of RHA/CBP complexes potentiated MR function, a transient expression assay using a luciferase reporter with MREs in the promoter was performed. Full-length and deletion mutant MR expression plasmids were cotransfected into 293T cells in the presence or absence of aldosterone. The results of this assay showed that the expression of RHA or CBP enhanced both AF-1a region transactivation and the aldosterone-induced transactivation function of full-length MR. RHA and CBP exhibited cooperative activity in transactivational enhancement of both AF-1a and full-length MR, which was consistent with the hypothesis that RHA and CBP act as part of the same coactivator complex. The lack of synergism between RHA and CBP in the AF-1a potentiation may be due to the relative abundances of the two factors. The transactivation functions of the AF-1b and AF-2 regions, which did not bind RHA, were not potentiated by RHA, while CBP and TIF2 potently coactivated AF-2 (Fig. 5).

Interaction with RNA polymerase II is not essential for MR transactivation by RHA. It has been reported previously that RHA directly interacts with RNA polymerase II through the minimal transactivation domain (MTAD) within the RHA molecule (4). However, RNA polymerase II was not detected in the glycerol density gradient fractions that contained the RHA/CBP complexes (data not shown). Therefore, using RHA mutants RHAΔMTAD and RHA W339A, which do not bind RNA polymerase II, we examined whether interaction between RHA and RNA polymerase II was required for the enhancement of AF-1a function by RHA/CBP complexes (4). Since both mutants were still functional, our results suggested that association between RNA polymerase II and RHA was not essential for RHA/CBP complex-mediated potentiation of AF-1a transactivation (Fig. 6).

RHA potentiates MR in a ligand-selective manner. Our results suggested that recruitment of RHA/CBP complexes to MR bound to target gene promoters was ligand selective. Therefore, we next investigated whether RHA/CBP complexes potentiated MR in a ligand-selective manner. In agreement with previous results, RHA was active only for aldosterone-bound MR (Fig. 7A). An MR mutant that lacked the AF-1a region (MRΔAF1a) lost potentiation of aldosterone-induced transactivation by RHA (Fig. 7B). Thus, aldosterone binding to MR may induce an altered conformation of the A/B domain, which would then result in increased access of RHA/CBP complexes to the A/B domain. In contrast, the AF-1a region of hydrocortisone-bound MR may be in a conformation that blocks RHA/CBP complex association.

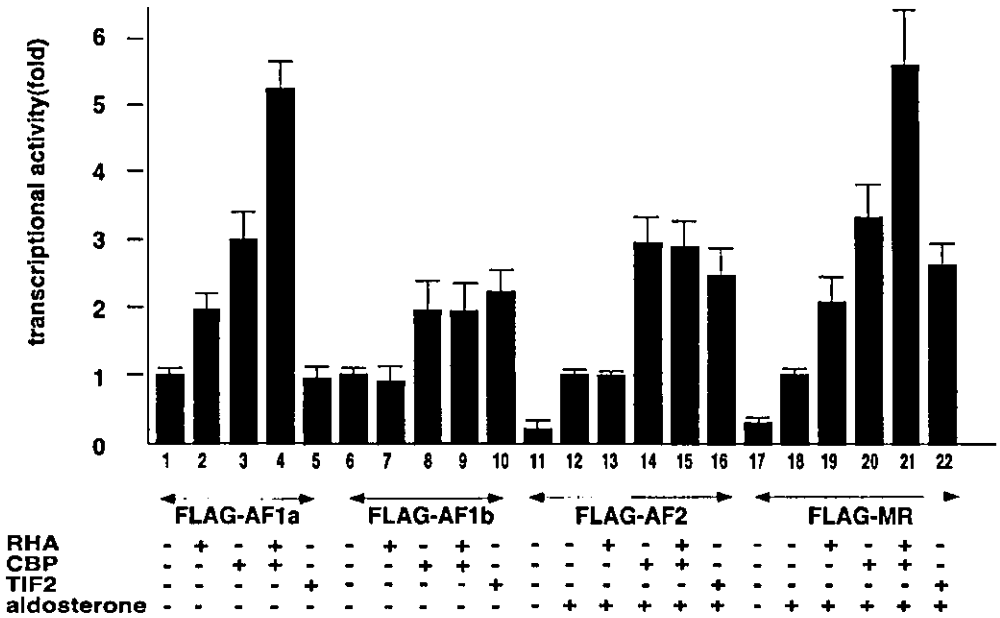

FIG. 5. RHA and CBP cooperatively potentiate AF-1a and aldosterone-bound MR. 293T cells were cotransfected with 0.25 μg of a luciferase reporter plasmid bearing progesterone response elements (PREx2-tk-luc), 50 ng of an expression vector containing an MR deletion mutant tagged with FLAG, and 0.3 μg of either pc-DNA, pc-DNA-HA-RHA, pc-DNA-CBP, or pc-DNA-TIF2 in the presence (+) or absence (−) of aldosterone (10^{-9} M). Bars show the fold change in luciferase activity relative to the activity of the MR deletion mutant (in the presence of 10^{-9} M aldosterone) or the activity of pc-DNA-FLAG-MR-FL (in the presence of 10^{-9} M aldosterone) without transfection of coactivators.

DISCUSSION

The A/B domain is poorly conserved among the members of the nuclear receptor superfamily, and the function of the A/B domain in terms of ligand-induced transactivation and coactivator action is not fully understood. In a previous study, we reported that the rat MR A/B domain harbored two AF-1 regions, designated AF-1a and AF-1b. While AF-1b and AF-2 activities were enhanced by TIF2 and CBP/p300, AF-1a activity was potentiated by CBP/p300 but not by TIF2 (16). Therefore, it was thought likely that AF-1a was potentiated by different coactivator complexes that contained CBP/p300 rather than TIF2. In the present paper, we have shown that the RHA/CBP complex acts as a coactivator of AF-1a activity. Glycerol density gradient analysis showed that RHA and CBP were present in fractions that possessed high HAT activity and were likely to contain multiprotein complexes of more than 670 kDa. Together with our previous observation that TIF2 was unable to potentiate AF-1a function, our present study suggests that RHA/CBP complexes probably contribute, at least in part, to the observed HAT activity of AF-1a-bound protein fractions (37).

RHA has been reported to be a component of the holoenzyme complex with RNA polymerase II, as well as to interact with CBP (36). In agreement with this previous study, RHA cosedimented with CBP in the same glycerol density gradient fractions, and RHA potentiated the interaction between CBP and the AF-1a region, leading to enhanced CBP-stimulated AF-1a activity. However, in contrast to the findings of previous studies (4, 12, 36), RNA polymerase II was not detected in the glycerol density gradient fractions that contained RHA and CBP (data not shown). Furthermore, the potentiation of AF-1a function by RHA mutants that lacked the putative interacting region for RNA polymerase II was comparable to that by wild-type RHA, which indicated that the RHA coactivator function for MR AF-1a required CBP but did not require direct association with RNA polymerase II.

SDS-PAGE analysis revealed that several proteins cosedimented with RHA and CBP. Unfortunately, the mass fingerprinting method we employed was unable to identify these other proteins. The failure to ascertain the identity of these other RHA/CBP complex components may be due to their relatively low abundance. Given the fact that MR AF-1a-associated complexes exhibited a broad spectrum of molecular weights within the glycerol density gradient fractions, it is likely that AF-1a-interacting complexes other than the RHA/CBP complex exist in the nucleus. Given the observed sizes of the HAT complexes on the glycerol density gradient, only some of the AF-1a-associated proteins appear to form the RHA/CBP complex.

Comparison of the crystal structures of ligand-binding domains from several nuclear receptors revealed that cognate ligand binding induced the repositioning of the C-terminal α-helical structure (H12) to form a hydrophobic groove, which then served as an interaction surface for AF-2 coactivators (7, 9, 18). We have previously shown that for the vitamin D receptor, some synthetic ligands can induce different H12 configurations that create recognition surfaces for the ligand-selective recruitment of various coactivators (47). However, GST pulldown and luciferase assays using MR and known AF-2 coactivators failed to detect ligand-selective coactivator re-